ADDIS ABABA UNIVERSITY

ADDIS ABABA INSTITUTE OF TECHNOLOGY

SCHOOL OF CIVIL AND ENVIRONMENTAL ENGINEERING

Assessing and Analyzing Ballast Flying and its Influence (Case Study of Addis – Adama Project)

Fikadu Mengistu

Advisor: Dr.Ing. Henok Fikre

A Thesis in Civil and Environmental Engineering in Railway Stream

Addis Ababa University

Addis Ababa, Ethiopia

July 2017

Assessing and Analyzing Ballast Flying and its Influence (Case Study of Addis – Adama Project)

Fikadu Mengistu

A Thesis Submitted to

The School of Civil and Environmental Engineering

Presented in Fulfilment of the Requirements for the Degree of Master of Science

(Civil and Environmental Engineering)

Addis Ababa University

Addis Ababa, Ethiopia

July 2017

ADDIS ABABA UNIVERSITY

ADDIS ABABA INSTITUTE OF TECHNOLOGY

SCHOOL OF CIVIL AND ENVIRONMENTAL ENGINEERING

This is to certify that the thesis prepared by Fikadu Mengistu, entitled: Assessing and Analyzing Ballast Flying and its Influence (Case Study of Addis – Adama Project) and submitted in partial fulfillment of the requirements for the degree of Master of Sciences (Civil and Environmental Engineering) compiles with the regulations of the University and meets the accepted standards with respect to originality and quality.

Approved by the Examining Committee:

Internal Examiner _____ Signature _____ Date _____

External Examiner _____ Signature _____ Date _____

Chair Mr. Mequanent Mulugeta Signature _____ Date _____

Advisor Dr.Ing. Henok Fikre Signature _____ Date _____

_____

School or Center Chair Person

UNDERTAKING

I certify that research work titled “Assessing and Analyzing Ballast Flying and its Influence (Case Study of Addis – Adama Project)” is my own work. The work has not been presented elsewhere for assessment. Where material has been used from other sources it has been properly acknowledged / referred.

Signature of Student

Fikadu Mengistu

Abstract

One of the major problem in ballasted railroad is ballast flying and it should be studied and has to be minimized. Ballast flying is defined as the projection of ballast particles from its resting position as the train pass over the track structure. Ballast particles become airborne by overcoming gravity and friction (interlocking) forces from neighboring particles.

The primary objectives of this paper are to identify the behavior of the railway ballast flying and to suggest possible solutions by assessing the ballast flying risk possibility (Addis – Adama project) and by determining the major causes of ballast flying in the project mentioned above mainly using discrete element modeling.

Literatures have been thoroughly reviewed and the preliminary analysis were performed prior to the Discrete Element Method (DEM) analysis with a software Particle Flow Code (PFC). In this research modeling of the ballast material using PFC3D is done to get vibrational velocity of ballast used to construct from Addis to Adama project. The analysis is comprised of an impact load and ballast material behavior. Two types of gradation were used for the modeling and it shows different vibrational speed due to its mass.

Finally conclusions were made based on the result. The result of the discrete element modeling (DEM) shows that ballast maximum vibrational speed is 0.014m/s. Addis – Adama is double truck and the summation of the speed of two trains at their passing point is about 250km/h. A train having 300km/h can lift ballast if vibrational speed is 0.02m/s. The ballast vibrational speed used for Addis – Adama is less than 0.02m/s and there is no ballast flight in the network. Even though there is no ballast flying some precautions have to be done.

Keywords:

Ballast flying, Discrete element modeling, Ballast vibrational speed, Ballast mass

Acknowledgment

First of all, I would like to express my deepest gratitude to my advisor Dr. Ing. Henok Fikre, for his grateful motivation, guidance, support, continuous advice and constructive suggestions toward the completion of this thesis. I also thank Mr. Mequanent Mulugeta (MSc.) for giving supportive idea and consultation.

I also would like to thank Ethiopian Railways Corporation, which has supported me to study MSc. degree at Addis Ababa Institute of technology (AAiT).

Finally, I would like to thank my family being their when I need you the most. Your support and care is very helpful to finalize this thesis.

Table of Content

List of Figures

List of Tables

List of Abbreviations

CFD – Computational Fluid Dynamics

CCFD – Coupled Computational Fluid Dynamics

DEM – Discrete Element Modeling

FEM – Finite Element Modeling

PFC – Particle Flow Code

STL – Stereo lithography

Chapter One

1. Introduction

1.1. Background of the study

The railway track is composed of different layers of materials, the steel rails are laid on concrete sleepers that transmit the stress to the ballast layer which is the main load bearing stratum. Below the ballast a compacted sub-ballast or capping layer placed above the formation soil. The purpose of this railway track structure is to provide a stable, safe and efficient guided platform for the train wheels to run at various speeds with different axle loads. In order to achieve these objectives, the vertical and lateral alignments of track must be maintained and each component of the structure must perform its desired functions satisfactorily under various axle loads, speeds, environmental and operational conditions [1].

Track structures are exposed to cyclic loads so that the components of the rail track performance should be determined based on their fatigue life and better inspection and maintenance procedure could be set.

The ballast behavior is affected by different factors like Particle Characteristics, Aggregate Characteristics, Loading Characteristics and Particle Degradation property. To study this behaviors, different kinds of tests are available. Some of them are Los Angeles tests, Shape tests, Gradation and Unit Weigh tests. There are also other strength tests like triaxial test.

This thesis analyze the material property of the ballast flying used in the Ethiopian National Railway Project from Addis to Adama.

1.2. Statement of the problem

Many researchers have indicated that the major portion of any track maintenance budget is spent on substructure. Economic studies by Wheat and Smith [2] into British rail infrastructure showed that more than a third of the total maintenance expenditure for all railway networks that operate on ballasted track goes into substructure.

Railway authorities in the USA spend tens of millions of dollars annually for ballast and related maintenance [3], while the Canadian railroads have reported an annual expenditure of about 1 billion dollars, where most of which includes track replacement and upkeep costs [4]. Fast train lines such as the Shinkansen Line (Japan) and the TGV-Sud-Est Line (France) face even higher maintenance costs. The huge cost involved in substructure maintenance can be significantly reduced if thorough understanding of the physical and mechanical characteristics of the rail substructure and the ballast layer in particular is obtained.

The Ethiopian railway line will also face with the problems related to the ballast within some operational time. Some of them are the following:

- Ballast fouling
- Ballast settlement and
- Ballast flying

The main focus of this paper is to investigate the influence of ballast flying on Ethiopian National Railway project and suggest appropriate solutions.

1.3. Objective of the study

General Objective

The main objective of this research is to study the behavior of the railway ballast flying and to suggest possible solutions. Since the project is double track and other additional factors like wind speed, seismic activities and its dynamic load makes it susceptible for ballast flying, it should be studied in detail.

Specific Objectives

- To assess the ballast flying risk possibility for Addis – Adama project specifically
- To determine the major causes of ballast flying in the project mentioned above
- To suggest for the possible solutions

1.4. Scope of the Study

The scope of this research is the investigation of ballast flying property and suggesting the possible measures to be taken after investigation. But as a track structure the ballast should be studied as a ballast material and as the whole track structure. Because every component condition affects other components. The software used here was a student version and limited by size. Due to this ballast layer is only considered.

1.5. Thesis Outline

Chapter One: Introduction

Chapter Two: Literature review – presents a comprehensive literature review that provides insight into the current state of knowledge and identifies ballast flight risk factors.

Chapter Three: DEM Modeling – presents modeling of ballast material and get ballast vibrational speed. Particle Flow Code is used as a discrete element modeling.

Chapter Four: Conclusion and Recommendation – presents conclusion based on the modeling result and it recommends the possible solution.

Chapter 2

2. Literature Review

Railway transportation plays a great role in the growing economy of the world. Its huge carrying capacity with very low cost makes it preferable transportation mode. The speed of the rail is also getting very high which is becoming comparable with the airline speed. Railway is known by its limited use of space, reliability and safety, high degree of automation and management and its low environmental impact [8]. Rail track network forms an essential part of the transportation system of a country and plays a vital role in its economy. It is responsible for transporting freight and bulk commodities between major cities, ports and numerous mineral and agricultural industries, apart from carrying passengers in busy urban networks. In recent years, the continual competition with road, air and water transport in terms of speed, carrying capacity and cost have substantially increased the frequency and axle load of the trains with faster operational speeds [9].

The railway track is composed of different layers of materials, the steel rails are laid on concrete sleepers that transmit the stress to the ballast layer which is the main load bearing stratum. Below the ballast a compacted sub-ballast or capping layer placed above the formation soil. The purpose of this railway track structure is to provide a stable, safe and efficient guided platform for the train wheels to run at various speeds with different axle loads. In order to achieve these objectives, the vertical and lateral alignments of track must be maintained and each component of the structure must perform its desired functions satisfactorily under various axle loads, speeds, environmental and operational conditions.

2.1. Track System

There are two types of rail tracks; those are conventional ballasted track and slab track.

2.1.1. Ballasted Track

The conventional ballasted railway track system has different components, among those the rail and fastening system, sleeper, ballast, sub-ballast and sub-grade are the main components.

The following are the main advantages of a ballasted track:

- Relatively low construction cost and use of indigenous materials,
- Ease of maintenance works,
- High hydraulic conductivity of track structure, and
- Simplicity in design and construction.

The disadvantages are significant and are as follows:

- Degradation and fouling of ballast, requiring frequent track maintenance and routine checks,
- Disruption of traffic during maintenance operations,
- Reduction in hydraulic conductivity due to the clogging of voids by crushed particles and infiltrated fines from the subgrade,
- Pumping of subgrade clay and silt size particles (clay pumping) to the top of ballast layer particularly in areas of saturated and soft subgrade,
- Emission of dust from ballast resulting from high speed trains,
- Substructure becomes relatively thicker and heavier, which requires a stronger bridge and viaduct construction [9].

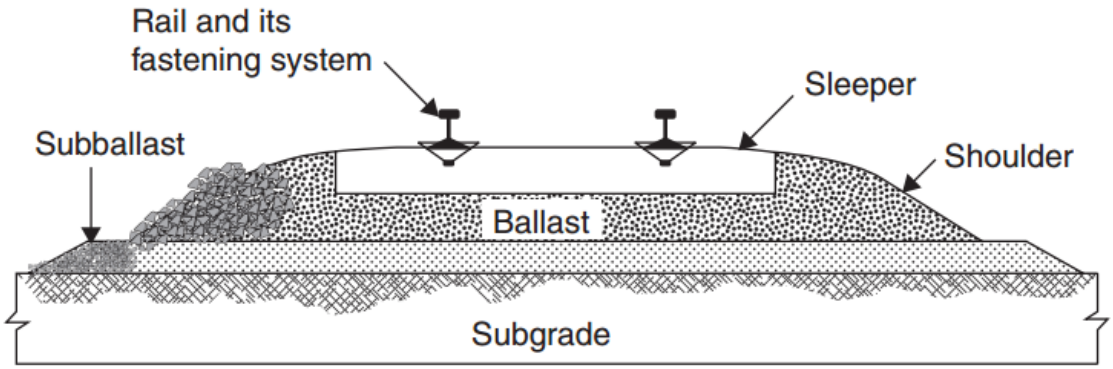

Figure 2.1: Track system structure [9]

2.1.2. Ballast

Ballast is the selected crushed and angular coarse aggregate materials placed above sub ballast to act as a load bearing platform to support the track superstructure (sleepers, rails). The sleepers are embedded into a ballast layer that is typically 250 – 350 mm thick.

Ballast behavior is governed by different factors as explained by Buddhima Indraratna et al [9]. The first factor is characteristics of constituting particles, which includes particle size, shape, surface roughness, particle crushing strength, resistance to attrition and so on. The second factor is bulk properties of the granular assembly including particle size distribution, void ratio or density and degree of saturation. The third factor is the loading characteristics. It includes the current state of stress, previous stress history and applied stress path. The fourth factor of ballast behavior is particle degradation, which is a combined effect of grain properties, aggregate characteristics and loading.

Functions of Ballast

Some of the functions of ballast are the following [9]:

- Provide a stable load-bearing platform and support the sleepers uniformly,
- Transmit high imposed stress at the sleeper/ballast interface to the subgrade layer at a reduced and acceptable stress level,
- Provide acceptable stability to the sleepers against vertical, longitudinal and lateral forces generated by typical train speeds,
- Provide required degree of elasticity and dynamic resiliency for the entire track,
- Provide adequate resistance against crushing, attrition, bio-chemical and mechanical degradation and weathering,
- Provide minimal plastic deformation to the track structure during typical maintenance cycles,
- Provide sufficient permeability for drainage,
- Facilitate maintenance operations,
- Inhibit weed growth by reducing fouling,

- Absorb noise, and
- Provide adequate electrical resistance.

2.2. Track Forces

Types of forces imposed on the track structure are classified as mechanical (static and dynamics) and thermal. These forces create vertical, lateral and longitudinal stresses. The static load is come from the total load of the train and its dynamic load is the interaction between rail vehicle wheels and the rails, which is a function of track structure, train characteristics (operating conditions) and other environmental conditions. Forces applied to the track are a combination of a static load and a dynamic component (which is superimposed on the static load). Temperature changes induce thermal stresses in the rail which cause expansion or contraction of the steel. Any restraint to the change in length, as in continuous welded rail, will set up internal stresses generally represented by a force acting in a longitudinal direction in the rail [10].

2.2.1. Forces Generated on Ballast Layer

Different types of loads are imposed on the ballast layer. The main load is the vertical load that come from the train load, which is a combination of a static load and a dynamic component superimposed on the static load. The static load is the dead weight of the train and superstructure, while the dynamic component, which is known as the dynamic increment, depends on the train speed and the track condition. During maintenance there is also tamping force which has been found to cause significant damage to ballast. There are also lateral and longitudinal forces on the ballast layer. The lateral force is the force that acts parallel to the long axis of the sleepers. The principal sources of this type of force are lateral wheel force and buckling reaction force. The longitudinal force is the force that acts parallel to the rails. The sources of this force are locomotive traction force including force required to accelerate the train, braking force from the locomotive cars and thermal expansion and contraction of rails [11].

2.2.2. Problems of Ballast

There are different types of substructure problems, among which ballast degradation, differential track settlement and ballast fouling are the prominent ones on the conventional track ballast. Ballast flying is one of the other problems which is occurred on the high speed track system. It is a limiting factor for the maximum allowed operational train speed.

2.3. Ballast Flying

2.3.1. Introduction

Ballast flying is defined as the projection of ballast particles from its resting position as the train pass over the track structure. Ballast particles become airborne by overcoming gravity and friction (interlocking) forces from neighboring particles. This phenomenon occurs when a combination of mechanical and aerodynamic forces, generated by the passage of the train, cause ballast particles to overcome gravity [1]. It is a complex interaction of different forces that cause the ballast flying to happen. This complexity arises from train aerodynamics, train dynamic load, track structure and the physical property of ballast.

Since 1980's, ballast flying became a known problem for high speed train due to aerodynamic force of the train. Different researchers tried to explain the concept of ballast flying and its causes that lead to the initiation and final projection of the ballast. Full scale experiment on the actual filled, wind tunnel test simulation and numerical test have revealed the major causes of ballast flying.

Different kinds of damages has been reported due to ballast flying. Damaged wheels, broken glasses at station, damaged speed limit sign around tunnel, distorted train under body structures, ballast pitting (railhead damage) and also injuries to maintenance staff have been reported. Due to these major maintenance costs and safety concern, ballast flying has been a great limitation of high speed rail for several decades.

2.3.2. Mechanism of Ballast Flying

Analysis of the data and modelling suggest that neither mechanical forces nor aerodynamic forces in isolation are likely to be sufficient to initiate ballast flight under the conditions investigated, but that the phenomenon could arise from a combination of the two effects [3].

The probabilistic occurrence of a ballast flight event is modeled as a combination of two sub-events – the displacement of ballast particles and the ballast flight given the displacement. The likelihood of ballast displacement is affected by the atmospheric conditions and ground conditions, while atmospheric, track, ground and aerodynamic forces contribute to the likelihood of ballast flight given a ballast displacement [1].

The risk of ballast flying can be expressed by the following expression

$$R_{fb} = P_d * P_{fb|d} * C$$

Where:

R_{fb} – ballast flying risk

P_d – the probability that a ballast particle will displace from its rest position

$P_{fb|d}$ – the conditional probability that a ballast particle will fly given the displacement

C – the consequence from the event of flying ballast

The mechanism of ballast flying is studied using high speed video recording of the ballast particles motion, wind tunnel tests in the laboratory and full scale experiment in the actual site. The field test is carried out by measuring the speed of wind and its pressure on the ballast particles using Pitot-static probes and the vibration of the sleeper and ballast particles measured by using geophones and accelerometer respectively.

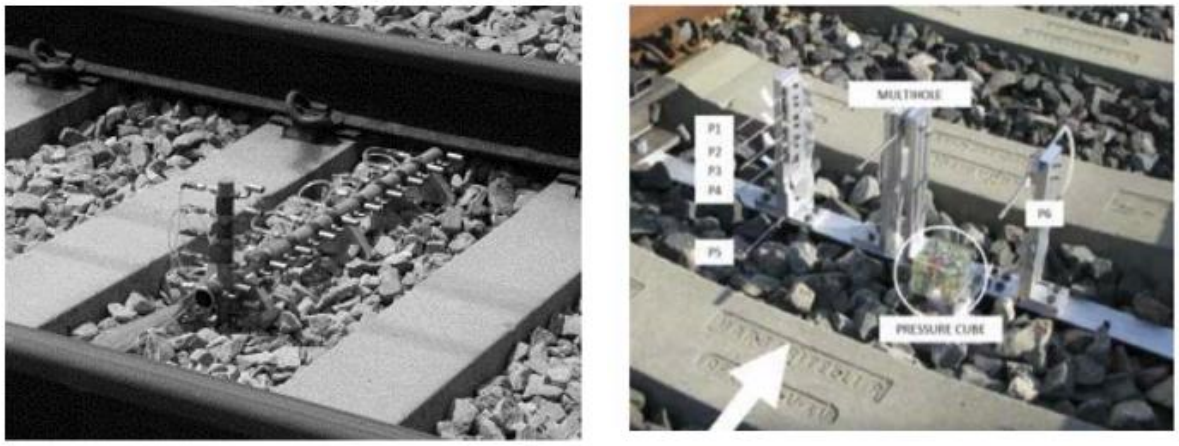

Figure 2.2: Arrangement of pitot static probes [1, 5]

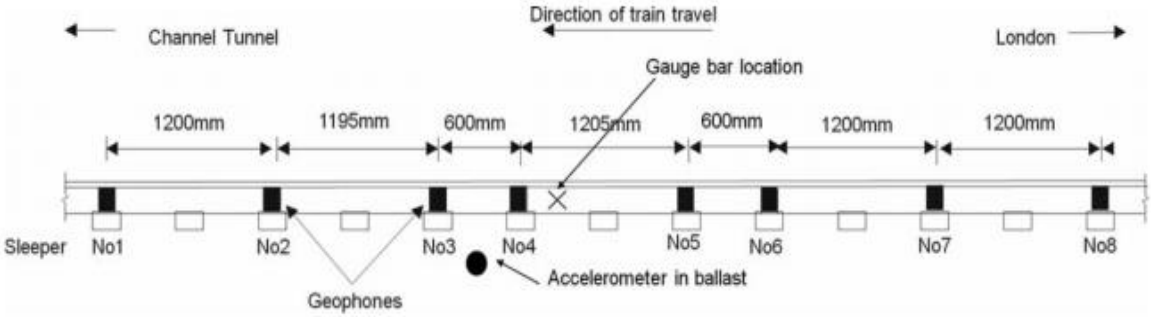

Figure 2.3: Position of geophones and accelerometers [3]

The next figure shows wind tunnel test. The ballast particles adhered to the platform in a row perpendicular to the wind direction, and the air pressure transducer adhered to the surface of ballast particle. The critical wind velocity (V_c) at which the ballast started to move were recorded when the wind velocity increased. Then the displacement of ballast were measured and recorded.

Figure 2.4: Laboratory wind tunnel test to measure critical wind velocity and displacement of ballast [2]

The ballast flying processes includes two stages, ballast initial motion and move with wind. Firstly the ballast particle is set in motion, and then followed by a longitudinal transport stage close to the ballast bed that is propelled by aerodynamic forces, and where the particle/particle contact actions play a dominant role. When the particle has reached sufficient longitudinal momentum, or the ballast particle stability balance is expired, the contact actions can lead to the particle gathering enough vertical momentum to initiate the ballast flying.

G.Q. Jing (etl…) [4] gave the detailed descriptions about the ballast flying mechanism using the following simple mechanics model to explain the main parameters.

Herein, the ballast particles are analyzed and characterized by the mg, F_i, F_w, a_T.

Where:

mg – is gravity force by mass,

F_i – is ballast particle interlock force,

F_w – is wind force resulted by high speed train acted on ballast effective surface (Ae), and

F_a – is ballast acceleration due to ballast bed vibration,

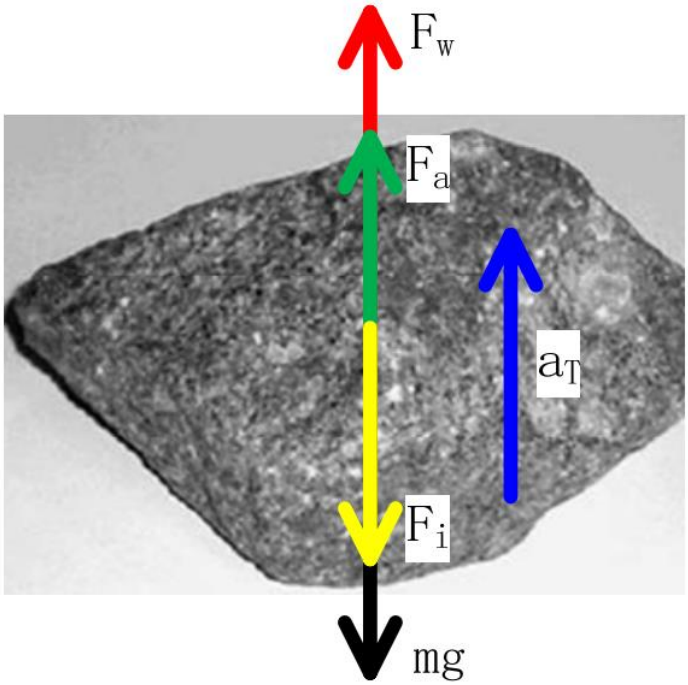

Figure 2.5: Forces acting on ballast [4]

Based on d'Alembert principle, the equation for ballast particle balance is (1)

$$F_w + F_a = mg + ma_T + F_i \quad (1)$$

Setting $F_i = 0$

$$ma_T = F_w - mg + F_a$$

$$ma_T = F_w - mg + ma = F_w - m(g - a) \quad (2)$$

Where a is ballast particle vertical acceleration caused by sleeper induced dynamic responses. Based on aerodynamics, the ballast particle force can be calculated by:

$$F_w = \int_0^A \int_{v1}^{v2} f(A) f(v) dA dv \quad (3)$$

Here:

A – wind loads effective area of ballast particle, and

*v*1, *v*2 – the points where the ballast particle interaction beginning and ending wind speed.

Due to wind speed calculation complexity, we usually take the wind pressure coefficient α, and then equation (3) becomes:

$$F_w = \alpha \int_0^A f(A) dA \quad (4)$$

Substituting equation 4 into equation 2

$$m a_T = \alpha \int_0^A f(A) dA - m(g - a) \quad (5)$$

$$a_T = \frac{\alpha \int_0^A f(A) dA}{m} - (g - a) \quad (6)$$

$$\frac{\alpha \int_0^A f(A) dA}{m} \quad (7)$$

a_T - indicates the particular ballast particle state of balance,

If $a_T < 0$ it indicates the ballast particles are stable and free of ballast flying,

$a_T = 0$ it indicates the ballast particles are in the critical state of stability, the train speed is a critical speed,

$a_T > 0$ it indicates the possibility of ballast flying phenomena.

$(g - a)$ – It is a constant value for ballast particles under certain train and track conditions which depends on ballast particle position, density and shape.

$\frac{\alpha \int_0^A f(A)dA}{m}$ – It is related with the wind load effective area, the ballast particle mass, ballast shape, ballast density, ballast size.

α – Wind pressure coefficient

The volume of ballast can be calculated with the integral of surface area multiplied with the thickness of the ballast

$m = \rho \int_{z1}^{z2} A(z)dz$ Where: ρ is density of ballast particle

$$a_T = \frac{\alpha f(A)}{\rho \int_{z1}^{z2} A(z)dz} - (g - a) \quad (8)$$

$$a_T = \frac{\alpha}{\rho \int_{z1}^{z2} dz} - (g - a) \quad (9)$$

Equation (9) shows the relationship between wind effects and vibration of ballast.

2.4. Factors That Contribute To Ballast Flying

There are many different factors for the projection of ballast particles. The interaction between train aerodynamics, train dynamic load, track response of ballast bed and sleeper, weather condition (wind load and snow accumulation) lead to ballast projection.

2.4.1. Train Aerodynamics

The pressure generated by the train on the ballast and the induced airspeed under the train are two aerodynamic effects that are very important. They are related with train speed, since the aerodynamic force is proportional to the square of the speed of the train [1]. Ballast flight have appeared to occur at speeds above 260 km/h. Other factors to take into account in this first risk factor are aspects related to the train design. A different nose configuration of the front of the train might be the key difference in experiencing flying ballast. One factor that is considered important by high speed rail (HSR) operators when attempting to characterize flying ballast is the length of the train. Studies performed in Spain as well as in Italy suggested that the length of the train played

a major role in the initial displacement of particles. It was noted that ballast flight was more likely to occur with a double-composition train – two separate train set units coupled to make up a longer train. This is due to the buildup of vortices underneath the car body of the train. One additional consideration related to speed is the effect of passing trains. There have been instances where a ballast stone was blown up when two trains travelling at speeds below 160 km/h. It was noted that the likelihood of ballast being displaced from its "at rest" position would dramatically increase as the speed of the train went above 260 km/h [6].

The ballast flying possibility increases non-lineally with train speed, for example, the Korea KTX ballast flying tests showed that the ballast flying possibility at 350km/h is twice of 300km/h [4]. Speed is one of the most important contributor to ballast flight risk.

The inter car gap has also great impact. It was noted that the presence of an inter car gap reduced the number of flying ballast particles as it provides an "escape door" to the highly turbulent airflow underneath the train.

2.4.2. Track Responses

It was noted that under certain loading conditions, the particles at the surface of the track would become weightless, meaning that the reacting forces applied to the particle would be large enough to overcome any gravity forces. The distances between wheel sets and between bogies can change the load input frequency to the track, thus causing different responses of the track. Field measurement of ballast acceleration using accelerometer and model results show that, with a speed of 260km/h and above, the acceleration experienced by the ballast particle exceed $10m/s^2$ which means that it causes weightless condition. Thus, an aerodynamic force would be sufficient to displace the particle [1, 3].

There are a number of mechanisms that may impose an upward velocity on the particle. These forces are due to both mechanical excitation (from train loading) and aerodynamic forces of the train. AD Quinn suggests the following reasons for initial upward velocity of the particles.

1. The movement of the entire ballast bed as the train passes over, causing an upward movement of surface ballast particles because of train loading/unloading effects (mechanical

vibration). From the field measurement data using geophone and accelerometer data, it is clear that train loading/unloading can account for initial velocities of the ballast particles.

2. An imbalance in pressure across the particle, with a low (or reduced) pressure on the particle upper surface and a higher pressure beneath it. Depending on both ballast particle size and train aerodynamic design, the pressure load has a considerable effect on the ballast to give initial upward velocity.

3. A vertical component of air velocity close to the surface of the ballast bed. The vertical velocity of the air could enhance the vertical velocity of the ballast particle.

An initial vertical velocity measured by the geophones and a vertical flow velocity field consistent with the maximum measured in the tests could start flight. The mechanical (geophone, accelerometer, and load cell) measurements showed that the ballast bed may experience significant train-induced forces, not related to aerodynamic factors, due to mechanical excitation of the track bed. Filtered measurements of sleeper and ballast velocity and acceleration showed that the ballast particles were unlikely to have sufficient velocity to become airborne due to mechanical vibrations alone. Unfiltered ballast accelerations of up to 20 m/s^2 were measured in relatively high frequency events, but it is not thought that these would last long enough to cause ballast particles to become airborne [3].

Distance between tracks also affect the track conditions. It is indicated that the distance between tracks plays an important role in ballast flight. The aerodynamic crosswinds created by two trains passing in opposite directions could produce a sufficient force to lift a ballast particle.

2.4.3. Surface Ballast Interlock Ability

Ballast flying can be reduced or eliminated with ballast particle interlock ability, especially the surface layer ballast particles. Several methods can be used to improve the ballast particle interlock force. The ballast bed compaction is a practical method; such as ballast bed well compacted, squeezed and pressed. From the ballast material characteristic part, the ballast surface roughness

or texture is considered to increase the ballast particle interlock or friction. The ballast specifications stipulated crushed or fractured ballast particles, which ask have a minimum 3 crushed fresh faces [4].

The 100 ballast particles interlock ability tests were conducted in site. Results showed that the ballast particle mass ranged from 34g to 185g, the interlock force ranged from 3.5N to 20.8N relied on self-weights and concrete positions. The interlock forces were within 20% of self-weight mostly, and 28 particles weighed bigger than 20%, while 9 particular weighed as high as 50% [4].

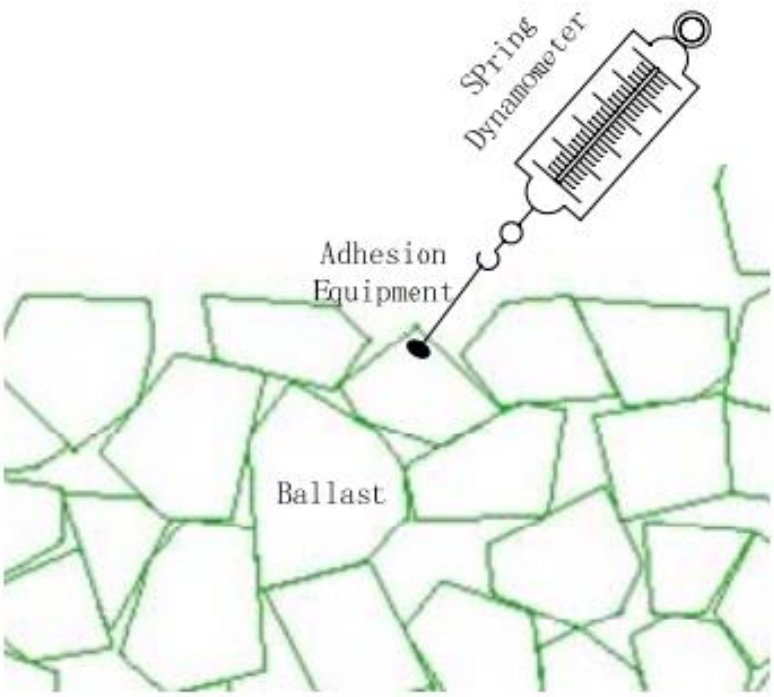

Figure 2.6: Interlock force survey [4]

2.4.4. Ballast Bed Vibration (Ground Condition)

It is important to consider the response of the sub-ballast and subgrade to loadings coming from the train as well as loadings produced by natural events, such as mild seismicity. Small magnitude earthquakes, while not felt directly by humans, can on the other hand produce an input ground motion to the ballast layer, thus causing some vibratory effects. Ballast flying is influenced by the ballast bed acceleration, with the ballast bed acceleration increase, the ballast flying possibility and severity improve. From the design or operation stages, we could alter the sleeper type, distance, fastener, rail or sleeper pad, ballast mat, ballast depth and density and so on. For example, increasing the sleeper mass and the rail pad elasticity, ballast mat application reduce the sleeper and ballast vibration. During ballast spreading or tamping, the ballast particles are easily fell on to the sleeper surface. In the cases, sleeper vibration is 10-20 times of ballast bed, far bigger than the gravity g, even if the train wind is very small, the ballast flying possibility is relatively higher than normal ballast bed case. China high speed railway ballast flying experience shows that, ballast flying possibly on bridges bigger than subgrade sections. Ballast bed vibration on bridges bigger than subgrade, and simultaneously, the wind gets stronger [4].

2.4.5. Ballast Shape and Mass

It is found that the size of the particle had a direct relationship with its likelihood to be picked up by winds. Specifically, the lower the ballast particle weighed, the higher the likelihood of the particle to be picked up by aerodynamic forces [1]. Ballast particle shape and ballast bed quality not only influence the resistance ability and stability, but also the ballast flying characteristics. For the same mass of ballast particles, the bigger efficient wind area, the higher ballast flying possibility [4]. It is found that the ballast particle displacement is partially inverse proportional to its mass.

2.4.6. Atmospheric Conditions

Atmospheric events might play a role in setting the right conditions for a particle to be picked up by a passing train. High winds blowing on the track could alter the arrangement of the particles laying on the surface of the track bed.

Ballast flying may occur by impact of accreted snow and ice from train under-floor. As the train travels in cold and freezing climates, ice can buildup in the covering region of the wheel set. When a train, for example, goes through a tunnel and experiences a temperature change, the ice may start melting, thus falling off the train.

2.5. Impacts of Ballast Flying

Obvious evidences of ballast flying such as damaging wheel, breaking glasses at station, and injuring acoustic screen have frequently been reported. The flying ballast particles may hit the bottom of train body and make it distorted. If the ballast fall onto the rail tread, the interaction between the wheel and rail surface may lead to derail for the worst case. Ballast flying is becoming an assignable factor of threatening the train operation and limiting the speed of ballasted high-speed trains.

Damage caused to the rail running surface (railhead) by trains is a major maintenance cost for any rail network. Various forms of railhead damage have been identified including rail breakage, traffic initiated wear, and fatigue-initiated surface cracks. Many of these are now collectively referred to as rolling contact fatigue, and mitigation measures include railhead surface grinding and lubrication. With the development of high-speed railways (HSRs), another form of railhead damage, known as ‘ballast pitting’, has become apparent. This form of damage seems to be associated with small particles of ballast becoming trapped between the railhead and the wheels of rail vehicles. On HSRs, it is thought that the speed and energy of the vehicle are sufficient to cause an explosive crushing of the ballast particle, which damages both the railhead and the wheel [3].

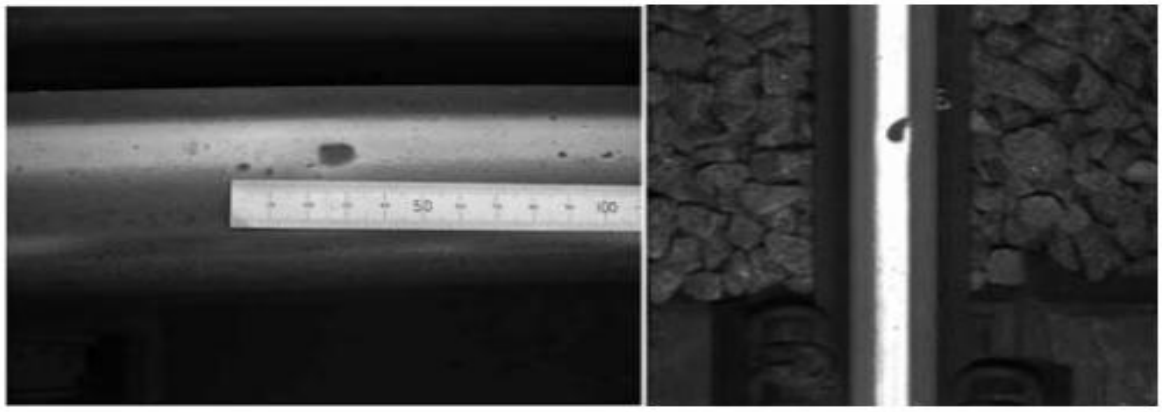

Figure 2.7: Ballast pitting [3]

2.6. Counter Measures to Reduce Ballast Flying

Different techniques are suggested by different researchers. Some of them are the following:

2.6.1. Slab Track

It can be a solution for ballast flying in constructing new high speed railway line, but due to high cost of slab track it cannot be a good solution. Ballasted track is still considered as the most cost-effective solution for not only conventional track but also for high speed railway operations.

2.6.2. Lowering the Ballast Profile

Lowering the ballast profile by 2 or 3 cm is a risk mitigation strategy adopted by several countries, such as France, Italy and Spain. The stones that are more prone to be picked up are the ones laying on the surface of the sleeper. By lowering the ballast profile voids are created between the bottom of the rail and the top of the ballast. Air that is compressed between the train and the track is now allowed to escape through these voids. The aerodynamic pressure is then reduced. This solution has showed to be a good solution in Italy and other countries [1].

The vertical distributions of averaged wind velocity shows that the average wind velocities at 200mm height from tie top were maximum about 40m/s and as the measurement points get lower, the average wind velocities decrease. The average wind velocity 20mm lower than the tie top (6.49m/s-18.56m/s) shows dramatic decrease relative to that 20mm higher than the tie top (24.59m/s-30.60m/s). This result implies that the blockage effect of the tie to the airflow induced

by train is very large and higher tie or lowered ballast surface can be good countermeasures to prevent ballast flying due to the strong wind during the passage of high speed train [5].

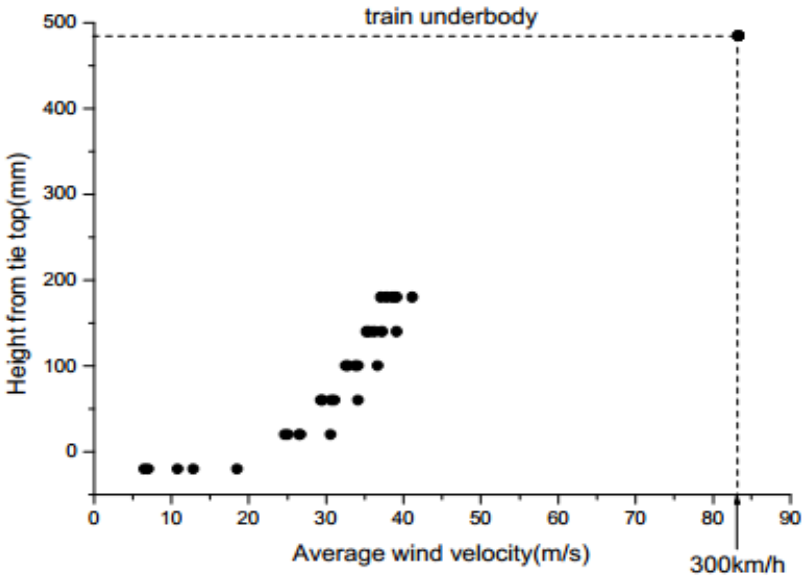

Figure 2.8: Vertical distribution of average wind velocity (at center of track) [5]

Le Pen and Powrie have undertaken research into the lateral sliding resistance of railway track and have investigated the relative contributions of base, crib and shoulder ballast. Their work suggests that friction between the sleeper/crib ballast interfaces is the mechanism that contributes between 37% and 50% of the total lateral sliding resistance, in combination with contributions from the crib and shoulder sleeper ballast interfaces. The inference is that increasing the ballast in the crib, above the sleeper tops, would not increase the lateral sliding resistance to any great extent. In addition, increasing the ballast shoulder height is much less effective at increasing lateral sliding resistance than increasing the shoulder width. This suggests that there are no good reasons for increasing the ballast height either alongside the track or between the rails.

2.6.3. Ballast Bagging

It is another risk mitigation strategy tested in Japan on those sections of the Shinkansen with ballasted track. The advantage of this solution is that the ballast particles are contained within the "bag", thus no ballast flight can occur. All the other functions of ballast are retained (drainage, lateral stability, stress distribution). The disadvantage is that the bags need to be removed and replaced for track maintenance [1].

Figure 2.9: Ballast bags placed on the Japanese Shinkansen [1]

2.6.4. Using Elastic Sleeper

GAO Liang et al [12] proved that by using elastic sleepers it could decrease vibration by approximately 30%. Vibration velocity and acceleration of ballast with elastic sleeper is smaller than that with conventional sleeper. This helps a lot to reduce ballast flying.

Table 2.1: Ballast vibration velocity [12]

Vibration Velocity/(mm.s^{-1})		
Depth/m	Elastic sleeper	Conventional sleeper
0.05	2.358	5.252
0.15	1.796	3.158
0.25	1.287	1.792
0.35	1.213	1.419

Table 2.2: Ballast vibration acceleration [12]

Vibration Velocity/(mm.s^{-2})		
Depth/m	Elastic sleeper	Conventional sleeper
0.05	2.083	3.264
0.15	1.409	1.759
0.25	0.676	1.103
0.35	0.666	1.084

It can be seen from the table that vibration velocity and acceleration of ballast under elastic sleeper is smaller than that under conventional sleeper.

Chapter 3

3. Discrete Element Modeling of the Ballast

3.1. Discrete Element Modeling (DEM)

In early 1970's, Cundall introduced the first computer program to model the progressive failure of a discrete block system. The interaction between blocks was governed by friction and normal stiffness. There was no limit to the amount of displacement or rotation of each block whenever blocks were touching or separated. It was designed for rigid body motion problems which were at that time impossible to be solved by finite element techniques. Cundall also described the basic theory of DEM, i.e., force-displacement law, law of motion, and computation cycles with time steps. Discrete Element Methods are numerical procedures to solve problems that exhibit gross discontinuous behavior. These methods are able to analyze multiple interacting bodies undergoing large dynamic movements. By modeling the individual particles and computing their motion, the overall behavior of the granular assembly is modeled implicitly. Interaction of granular materials or rock masses can this way be modeled accurately and realistically since any discontinuous detail can be included in the analysis. Discrete Element Methods have been widely applied to the soil and rock mechanics.

In the past years, researches on granular medium, especially numerical simulations, yielded significant results which can be applied to railway problems. DEM can be used to analyze a wide variety of mechanical properties of ballast bed (the microstructure of granular materials) that Finite Element Modeling (FEM) cannot. For example, the ballast settlement after long cyclic loading, distribution of particles contact force chains, ballast coordinate number, compactness, ballast vibration characteristics, breakage characteristics and lateral ballast resistance were investigated. DEM can reveal interaction between particles and structures with simple parameters. Furthermore, it takes into account geometry and physical properties of particles like dimension, contact attribute, dump, etc. Compared with FEM, DEM is not based on macroscopic continuity hypothesis, which is the main hypothesis of continuum mechanics. It combines microstructure of objects with their macroscopic mechanics. In DEM approaches, the material is modeled grain by grain as a discrete

system of rigid bodies in contact. During the evolution of the system, contact between grains can be created or disappear because of the motion of the grains. The interaction between grains follow laws of contact that can differ according to the DEM model [13].

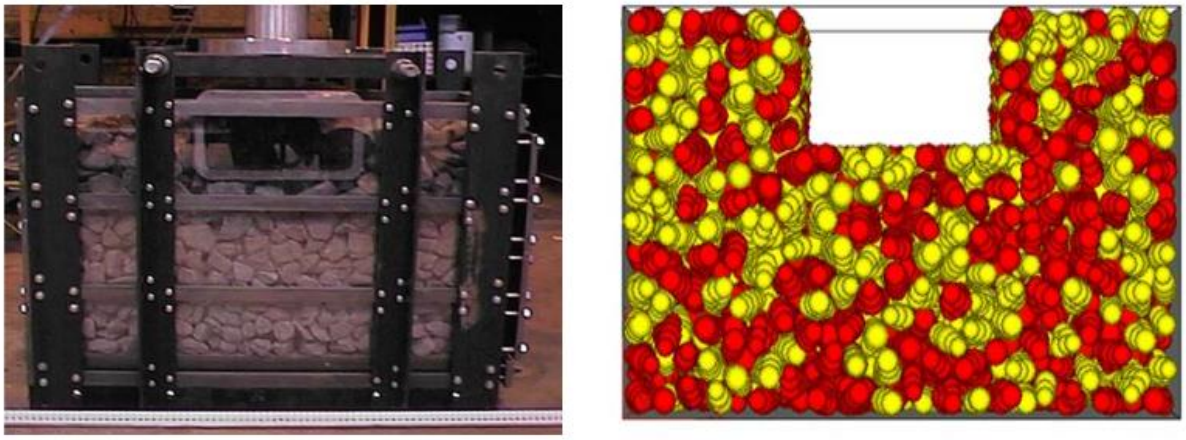

(a) (b)

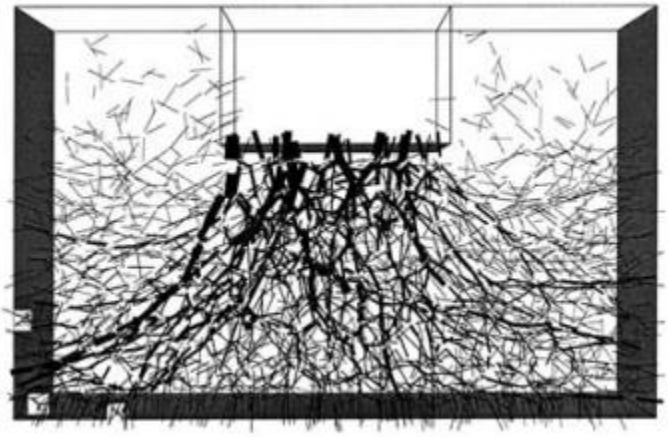

(c)

Figure 3.1: DEM Modeling [14]

(a) Box Test Sample, (b) DEM Simulation of Box Test, (c) Force Chains

Imaging technology can be used to obtain ballast shapes, which was then used to regenerate ballast in DEM. It helps to represent the actual shape of the ballast in the model. The figure shows ballast created by imaging technology.

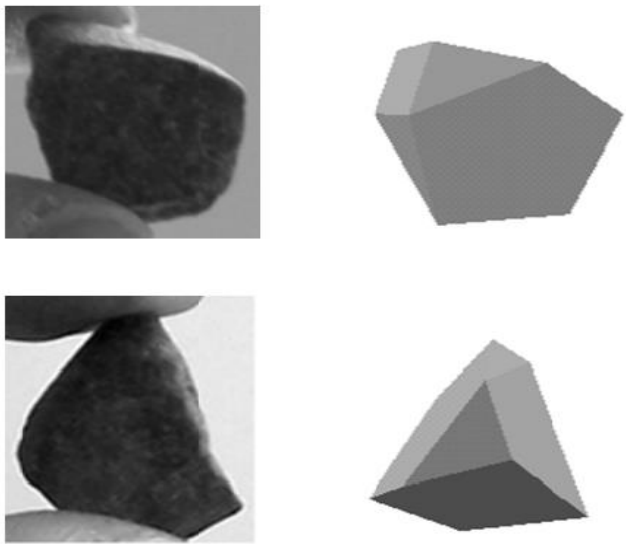

Figure 3.2: Using imaging technologies to model the actual ballast [15]

3.2. Particle Flow Code

Particle Flow Code (PFC3D/2D) software is a DEM software based on granular mechanics. It is suitable to analyze granular materials from a micro perspective. What is more, it allows users to simulate particles with simple spheres, and users can also establish model with sphere combinations that require users to exploit with FISH programming language. It is good at studying interaction and kinematic relation of complex particles.

The basic elements in PFC3D include sphere and wall. It is much easier to utilize sphere to model ballast, which can also save vast calculation time. However, sphere cannot represent multi-contact and interlocking characteristic of real ballast. So, cluster is used to model ballast by bonding spheres. Then, ballast breakage can be distinguished through broken bonds.

LU and McDOWELL concluded that when a cluster contains more than seven spheres, interlocking behavior of real ballast can be expressed well. Spheres in a cluster are bonded together. PFC3D provides two bonding models, a contact-bond model and a parallel-bond model. Both bonds can be envisioned as a kind of glue connecting two particles. However, there are also some obvious differences between the two bonding models. The contact-bond glue is of a vanishing small size that acts only on the contact points, whereas the parallel-bond is of an infinite glue that acts on a circular cross-section lying between spheres, which can represent the effects of additional material (e.g., cementation) deposits after the balls contact. When contact force exceeds bond strength, the bond breaks. There is no displacement between spheres when the bond exists [15].

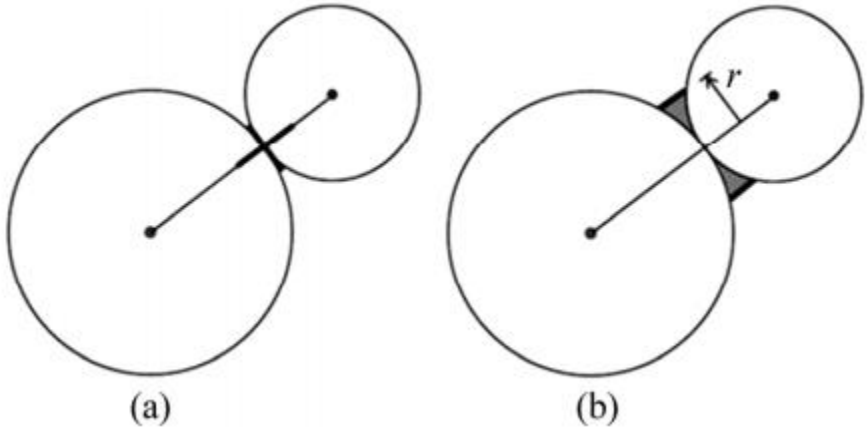

Figure 3.3: Two bonding models in PFC3D [15]

(a) Contact bond model; (b) Parallel bond model

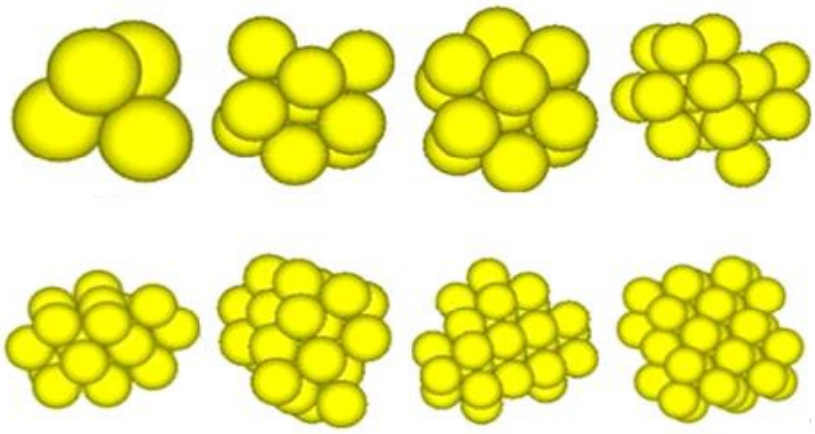

Figure 3.4: Models of ballast clusters using different number of balls. [15]

An accurate measurement of the contact forces and displacement is possible and sufficient micro-parameters data can be extracted for micro-mechanical analysis. PFC2D enables the investigation of features that are not easily measured in laboratory tests such as co-ordination numbers, inter-particle contact forces, and the distribution of normal contact vectors to be investigated, and it is also possible to compose bonded particles into agglomerates and simulate fracture when the bonds break.

The PFC programs (PFC2D and PFC3D) provide a general purpose, distinct-element modeling framework that includes both a computational engine and a graphical user interface. The PFC model simulates the movement and interaction of many finite-sized particles. The particles are rigid bodies with finite mass that move independently of one another and can both translate and rotate. PFC can be easily customized and applied to a very broad range of numerical investigations where the discrete nature of the systems is of interest. PFC has been successfully used for problems ranging from fundamental research on soil and rock behavior at the laboratory scale to slope stability and rock fall hazard mitigation, hydraulic fracturing, rock-tool interactions, bulk flow, mixing, conveying and compaction of aggregates and powders, blast furnace modeling, etc. [16].

The fundamental element in PFC is a disk with unit thickness in 2D and sphere in 3D. If the particles to be modeled have complex shapes, representing these shapes accurately may be important in the numerical model. There are two ways of representing blocky shapes with PFC. One method is by bonding two or more spherical particles together, forming a cluster. The spherical particles are rigid, but contacts are soft. Thus, the response of the assembly is studied by adjusting the parameters at the particle and contact levels; the constitutive behavior of the assemblage is derived automatically from the contact model and properties. The other is by using clumps to approximate complex shapes as collections of pebbles rigidly attached. A clump behaves as a rigid body. The inertia parameters of a clump can be automatically computed from the shape geometry or from the outer surface delineated by the pebble distribution or input by the user.

3.2.1. DEM Contact Bonds

In DEM two elements are in contact if the distance between the centers of two adjacent elements is equal to or less than the summation of their radii. The contact behavior is described using up to three models: slip, stiffness, and bonding. The slip model allows slipping to occur between discrete elements by limiting the shear force. The input parameter for this model is the friction coefficient (μ). The maximum allowable contact shear force is equal to the coefficient of friction multiplied by the normal force at that contact. The stiffness model relates the contact forces and relative displacement in the normal and shear directions (normal and shear stiffness).While the bonding model is a strength parameter above which a bond breaks. A contact bond works as a pair of elastic springs with normal and shear stiffness at the contact. In the first two methods, it is important to set these parameters to each group of aggregates before the simulation starts. If the magnitude of the tensile normal contact force equals or surpasses the normal contact bond strength, the bond will break. On the other hand, if the magnitude of the shear contact force equals or exceeds the shear contact bond, the bond will break [17].

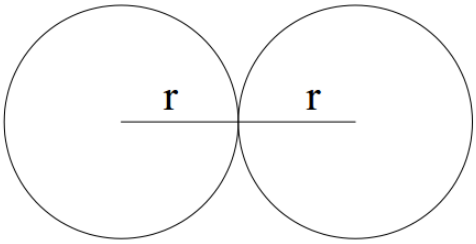

Figure 3.5: the distance between the centers of two adjacent elements in contact.

3.2.2. Calculation Cycle

The calculation cycle in PFC3D is a time stepping algorithm that requires the repeated application of the law of motion to each particle, a force-displacement law to each contact, and a constant updating of wall positions. The external loads are applied to the system by moving the walls with fixed velocities. The calculation cycle is illustrated in the following Figure.

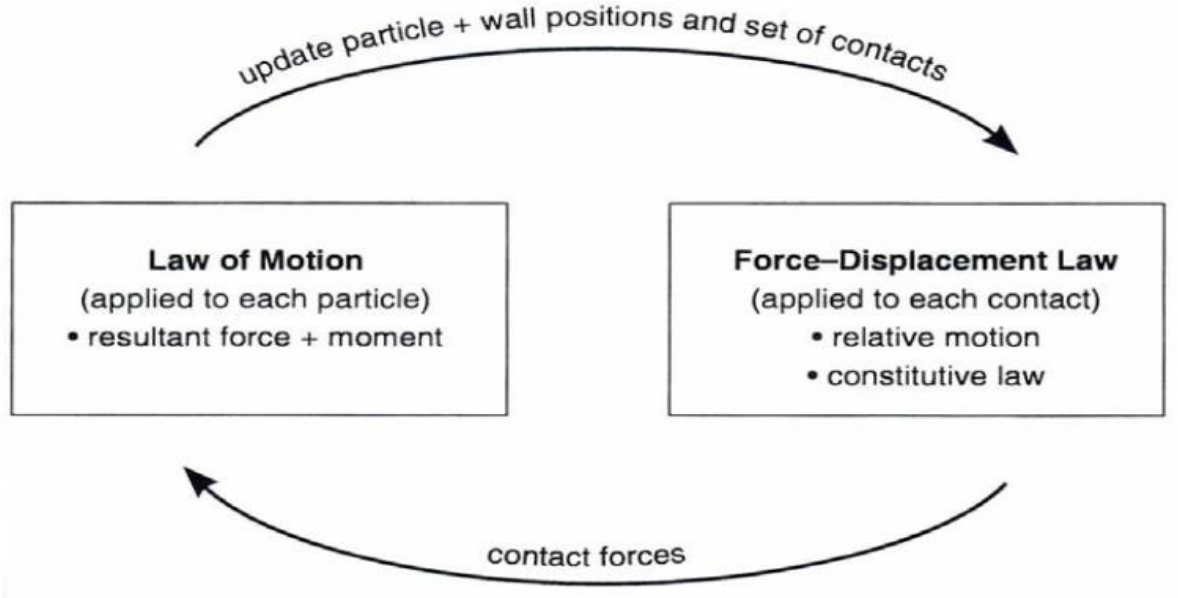

Figure 3.6: calculation cycle use in PFC3D (Itasca Consulting Group, Inc., 1999)

At the start of each time step, the set of contacts is updated from the known particle and wall positions. The force-displacement law is then applied to each contact to update the contact forces based on the relative motion between the two entities at the contact and the contact constitutive model. Next, the law of motion is applied to each particle to update its acceleration, velocity and position based on the resultant force and moment arising from the contact forces and anybody forces acting on the particle such as gravity. Lastly, the wall positions are updated based on the specified wall velocities. The force-displacement law at a contact is applied at the start of each cycle to each contact to obtain new contact forces. [11]

3.2.3. CCFD Add-on to PFC3D5.0

The Coupled Computational Fluid Dynamics (CCFD) add-on for PFC3D enables coupling the mechanical DEM calculation of PFC3D with a computational fluid dynamics solver. A solid modeler/post-processor called GiD is included with the computational engines. This package allows for interactive creation of arbitrary problem domains, and includes a volume and surface mesher. This package also allows the user to interact with a 3D view of the results.

To conduct a coupled problem, GiD is first used to build a GiD project file. This file describes the problem-domain geometry. The boundary and initial conditions of the fluid are also specified in GiD, along with timing information. The user develops a PFC3D data file to be invoked when the coupled calculation begins. The coupled calculation is started from within GiD via the *Calculate* dialog box. GiD starts CCFD, PFC3D and a proxy server that brokers communication between CCFD and PFC3D. During the coupled calculation, the proxy server controls PFC3D, and control is returned to PFC3D when the coupled calculation has ended. GiD is then used in post-process mode to view the results. Figure shows the organization of these components.

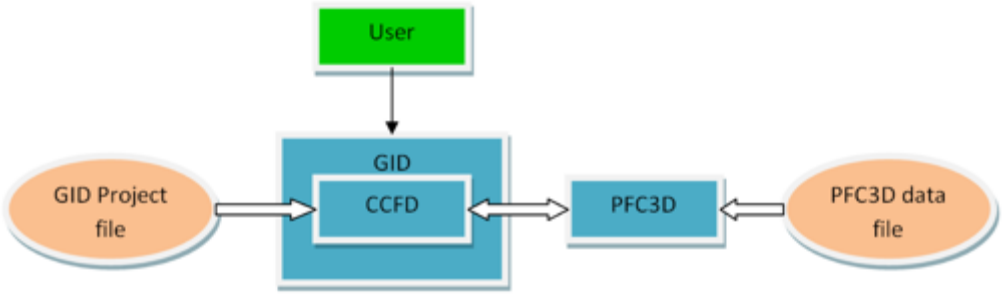

Figure 3.7: Organization of the CCFD option of PFC3D [16]

The Computational Fluid Dynamics (CFD) module allows some fluid-particle interaction problems to be solved in PFC3D. The CFD module does not contain a CFD solver. The CFD module is only available in the 3D version of PFC. The module provides commands and scripting functions to connect to CFD software and solve fluid particle interaction problems. Two-way coupling is realized by periodically exchanging this information between PFC and the fluid-flow solver. This module provides methods to:

- read a fluid mesh,
- store fluid velocity, fluid pressure, fluid pressure gradient, fluid viscosity and fluid density in each fluid element,
- calculate porosity and
- Automatically apply fluid-particle interaction forces to particles during PFC cycling.

3.3. Modeling

The ballast material of the Addis – Adama track was modeled using PFC3D/2D. The shape of the aggregate can be represented using different technic. PFC can represent the shape by forming clumps of balls. Clumps can be created using AutoCAD software. Using AutoCAD a 3D shape of aggregate is drawn and exporting the file to '**.stl**' format that can be read by PFC. Clumps can be created by bonding different number of balls. The following figures shows different shapes of aggregate using clumps.

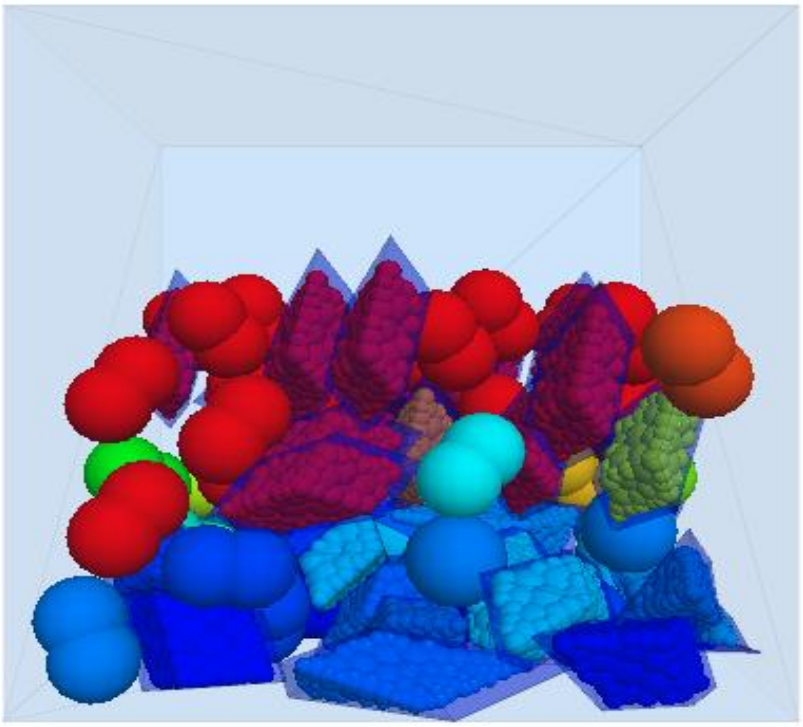

(a)

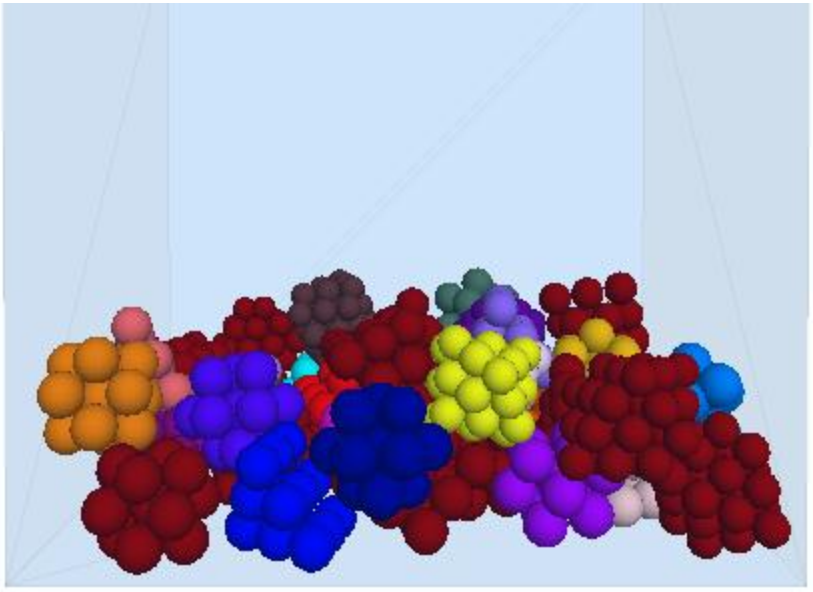

(b)

Figure 3.8: Spherical and angular shape representation of aggregates using PFC3D

3.3.1. PFC3D Modeling of the Ballast Sample

The Addis (Sebeta) – Adama Section of the new standard-gauge railway in Ethiopia is a double-track railway, which is 110.5km long with the designed maximum passenger train speed of 160km/h. It is a standard gauge (1435mm).

Table 3.1: Technical Standards of Addis Adama

Scope	Addis Ababa (Sebeta) – Adama
Gauge	1435mm
No. of main line	Double track
Target speed value	Passenger 160km/h
Distance between lines	4.0m

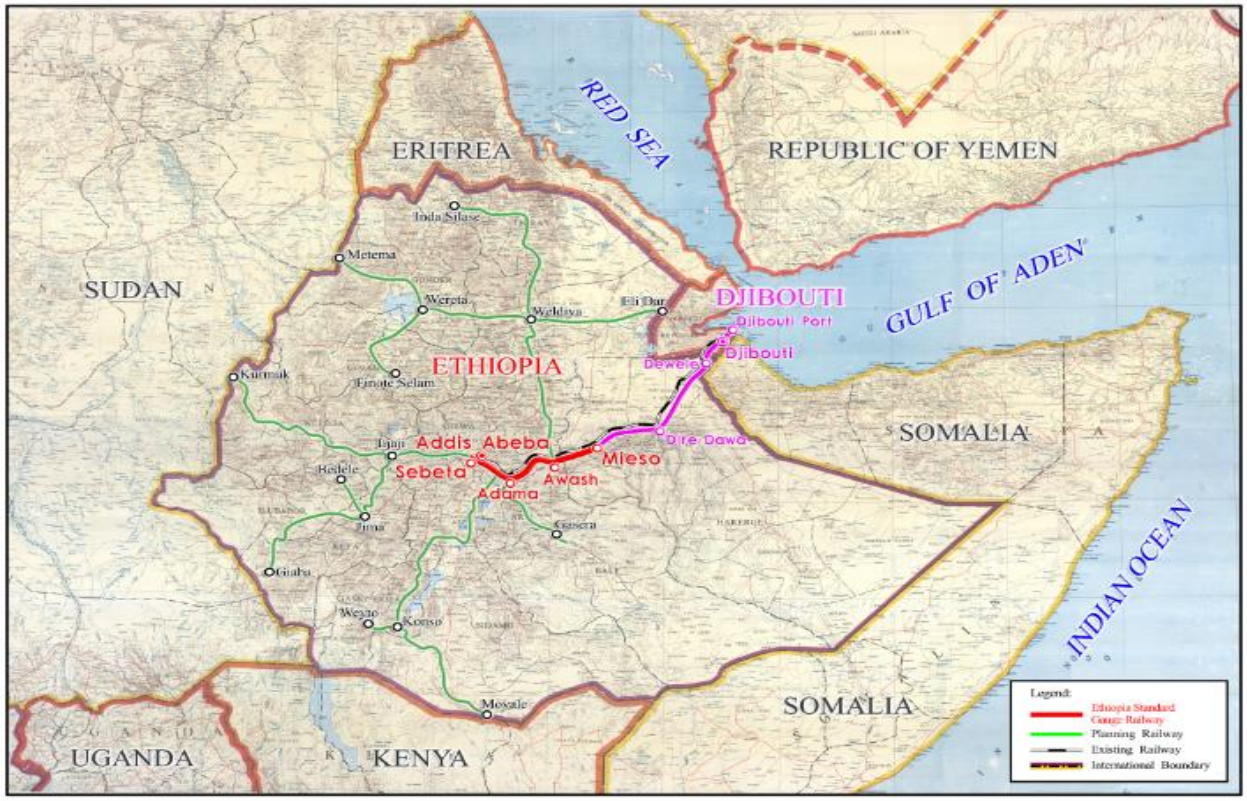

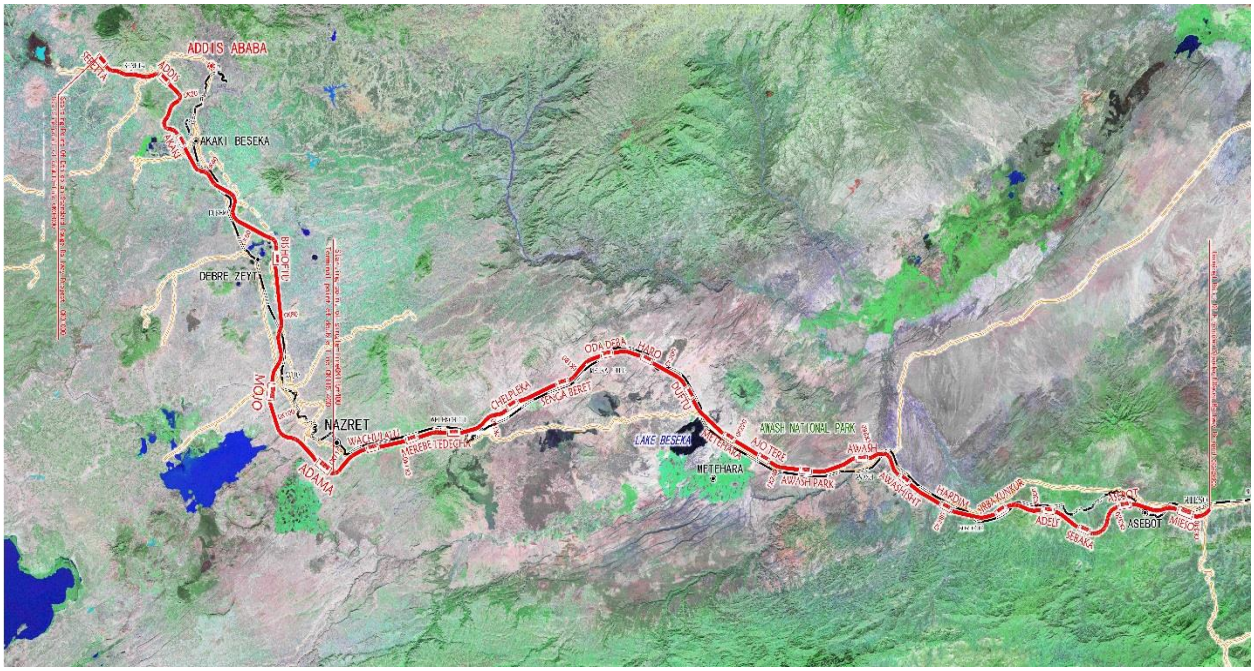

Figure 3.9: Addis – Addama – Djibouti line

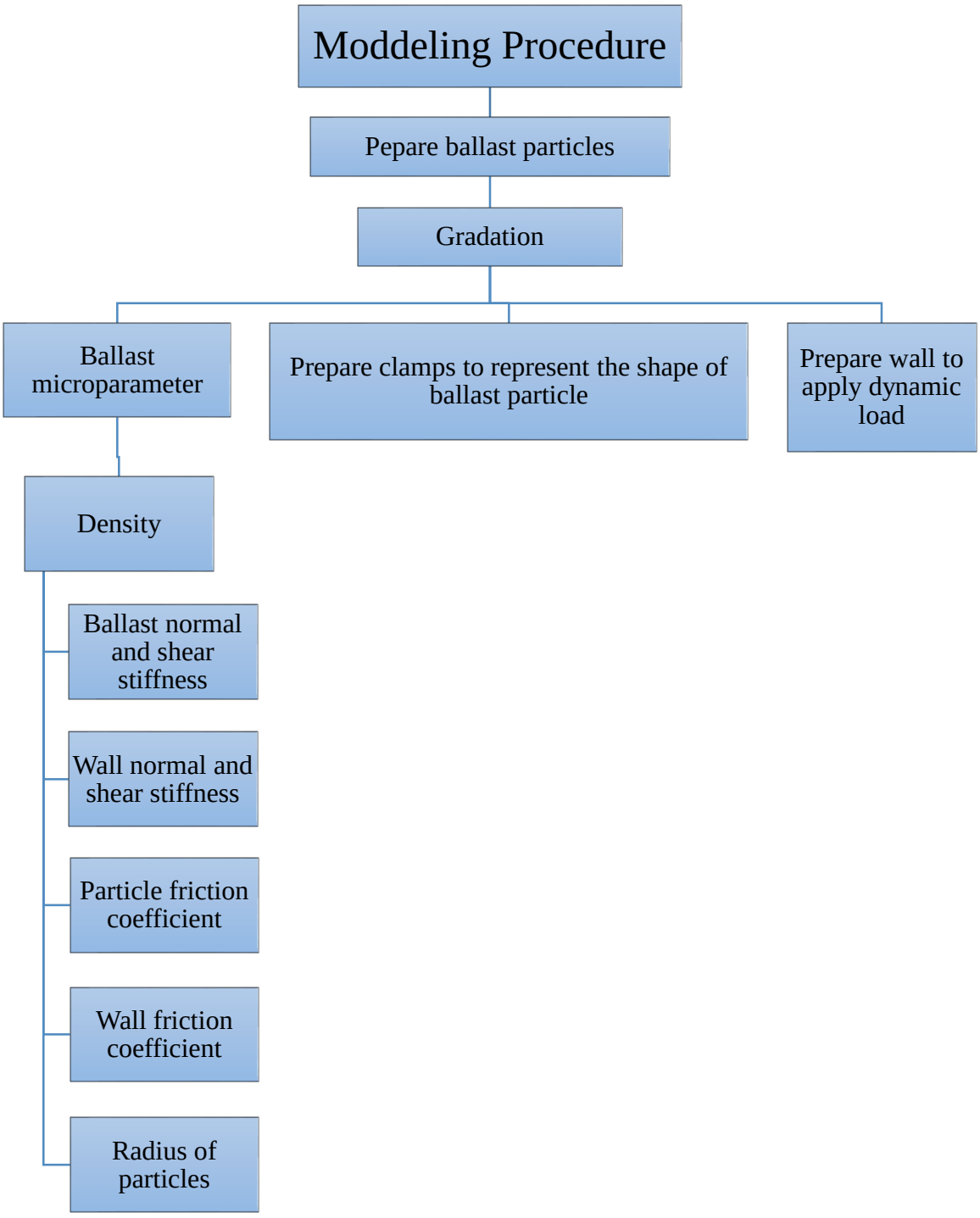

Figure 3.10: Modeling Procedure

Ballast gradation used is as follow:

Table 3.2: Particle size distribution

Sieve Size	Lower bound	%passing	Upper bound
63	97	99	100
56	92	95	97
45	55	73	75
35.5	25	37	40
25	5	9	15
16	0	0	5

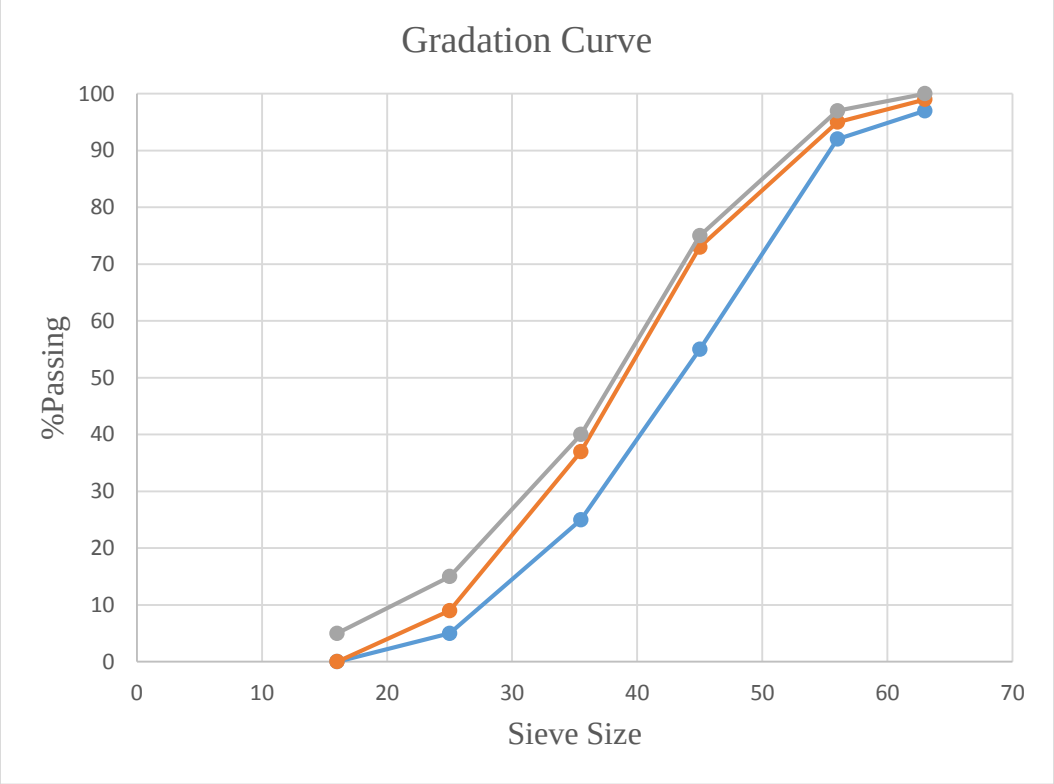

Figure 3.11: Particle size distribution

The sample produced using PFC3D and its particle size distribution looks like the following.

Table 3.3: Particle Size Distribution

Fraction (mm)	Mass %	Cumulative
16-25	9	9
25-35.5	28	37
35.5-45	36	73
45-56	22	95
56-63	4	99
63-70	1	100

Table 3.4: Upper Bound

Fraction (mm)	Mass %	Cumulative
16-25	5	5
25-35.5	20	25
35.5-45	30	55
45-56	37	92
56-63	5	97
63-70	1	100

Table 3.5: Lower Bound

Fraction (mm)	Mass %	Cumulative
16-25	10	5
25-35.5	25	15
35.5-45	35	40
45-56	22	75
56-63	3	97
63-70	0	100

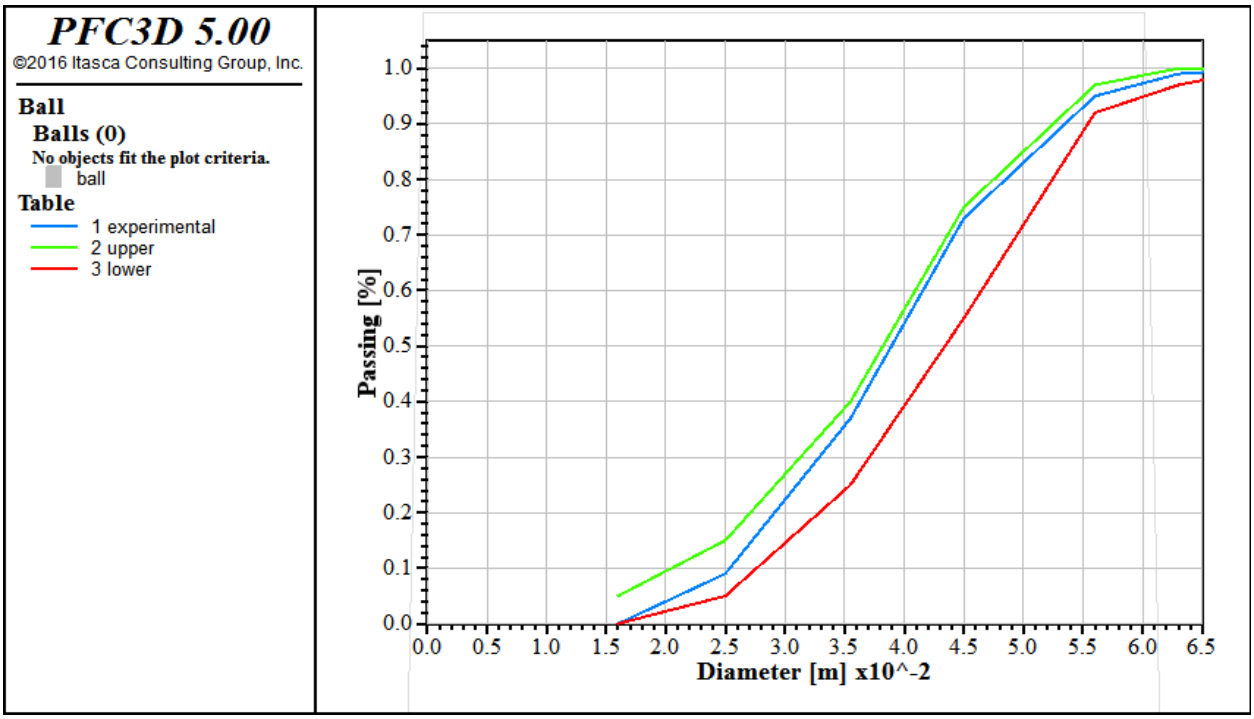

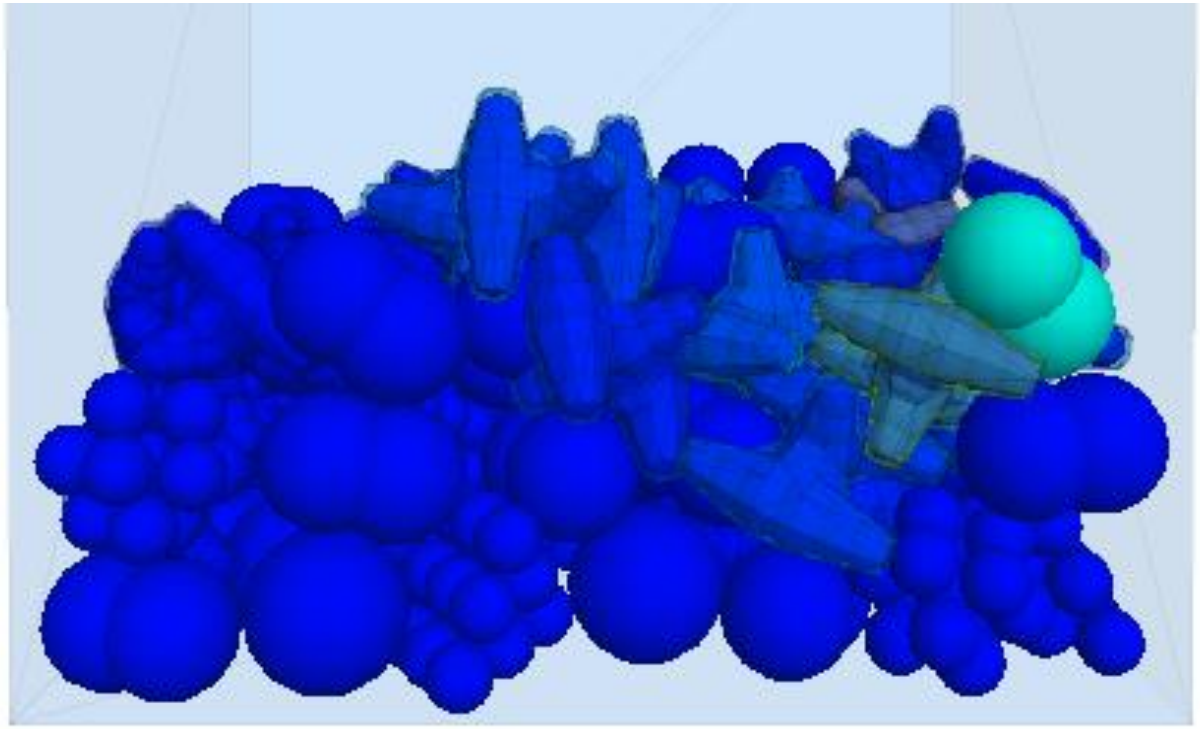

Figure 3.12: Particle Size Distribution Using PFC3D

Table 3.6: Parameters [12]

Micromechanics Parameters	Values
Ballast density (kg/m^3)	2600
Ballast particle normal and shear contact stiffness (N/m)	1*10^8
Wall normal and shear contact stiffness (N/m)	1*10^9
Particle friction coefficient	0.5
Wall friction coefficient	0.5
Radius of particles (mm)	22.4-63

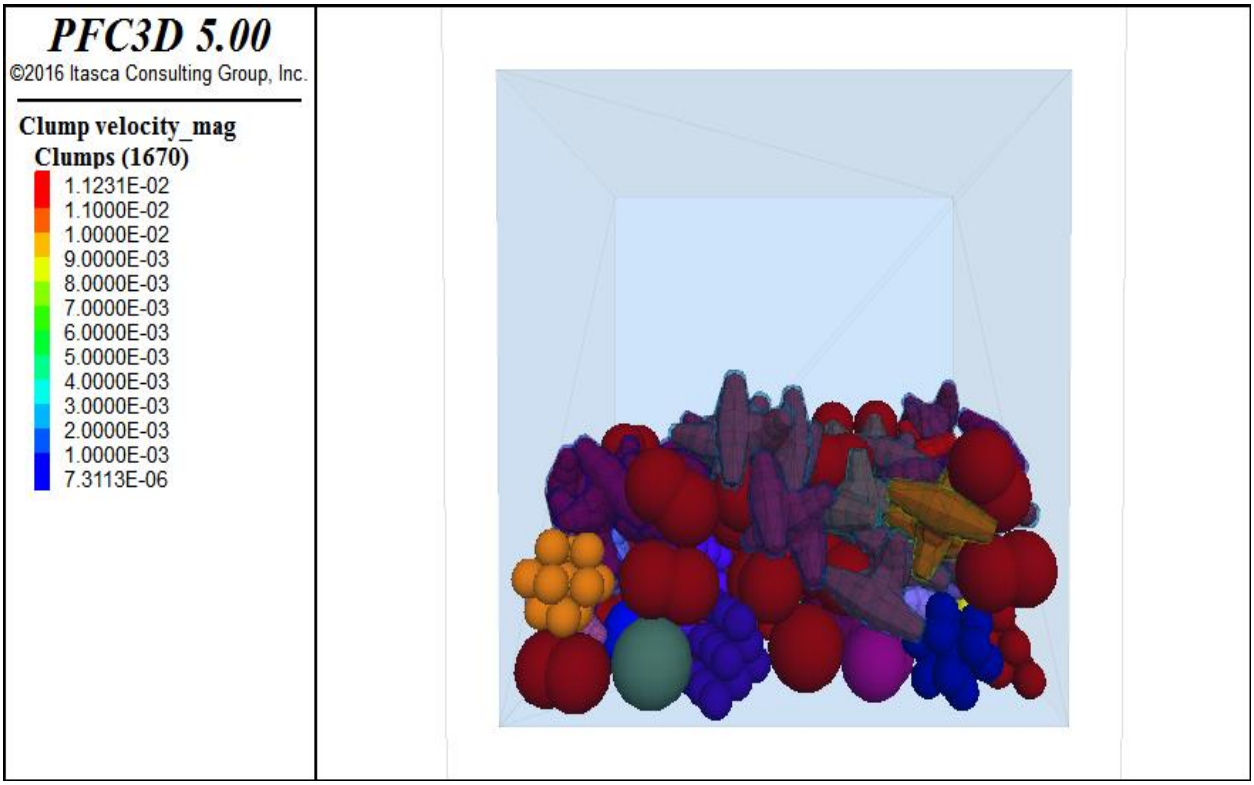

Figure 3.13: PFC3D Modeling Result

The maximum vibrational velocity is 0.011m/s as shown on the modeling.

3.4. Effect of Fouling Ballast Particles on Ballast Flying

Fouling is the term used to indicate contamination of ballast by the presence of fines. The fine particles have small weight surface area ratio. Due to this the particles easily picked up by aerodynamic force. The vibrational speed is also higher than bigger particles. Ballast gradation used is as follow:

Table 3.7: Particle size distribution

Sieve Size	Lower bound	%passing	Upper bound
63	97	100	100
56	92	96	97
45	55	74	75
35.5	25	39	40
25	5	14	15
16	0	3	5

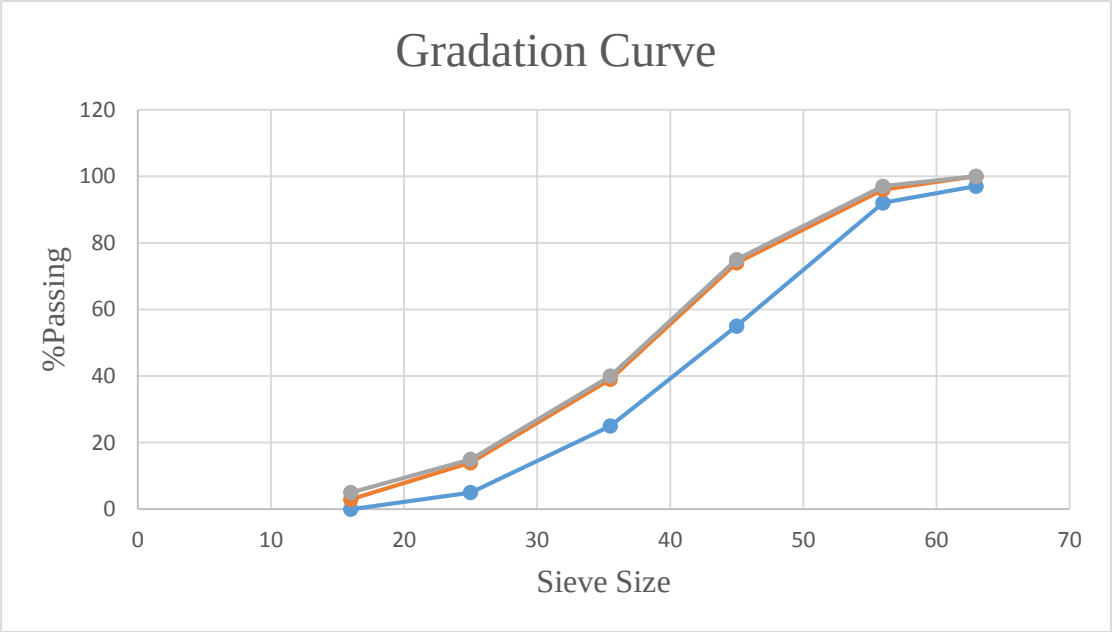

Figure 3.14: Particle size distribution

Table 3.8: Parameters

Micromechanics Parameters	Values
Ballast density (kg/m^3)	2600
Ballast particle normal and shear contact stiffness (N/m)	1*10^8
Wall normal and shear contact stiffness (N/m)	1*10^9
Particle friction coefficient	0.3
Wall friction coefficient	0.3
Radius of particles (mm)	16-63

The sample produced using PFC3D and its particle size distribution looks like the following.

Table 3.9: Particle Size Distribution

Fraction (mm)	Mass %	Cumulative
16-25	14	14
25-35.5	25	39
35.5-45	35	74
45-56	22	96
56-63	4	100
63-70	0	100

Table 3.10: Upper Bound

Fraction (mm)	Mass %	Cumulative
16-25	5	5
25-35.5	20	25
35.5-45	30	55
45-56	37	92
56-63	5	97
63-70	1	100

Table 3.11: Lower Bound

Fraction (mm)	Mass %	Cumulative
16-25	10	5
25-35.5	25	15
35.5-45	35	40
45-56	22	75
56-63	3	97
63-70	0	100

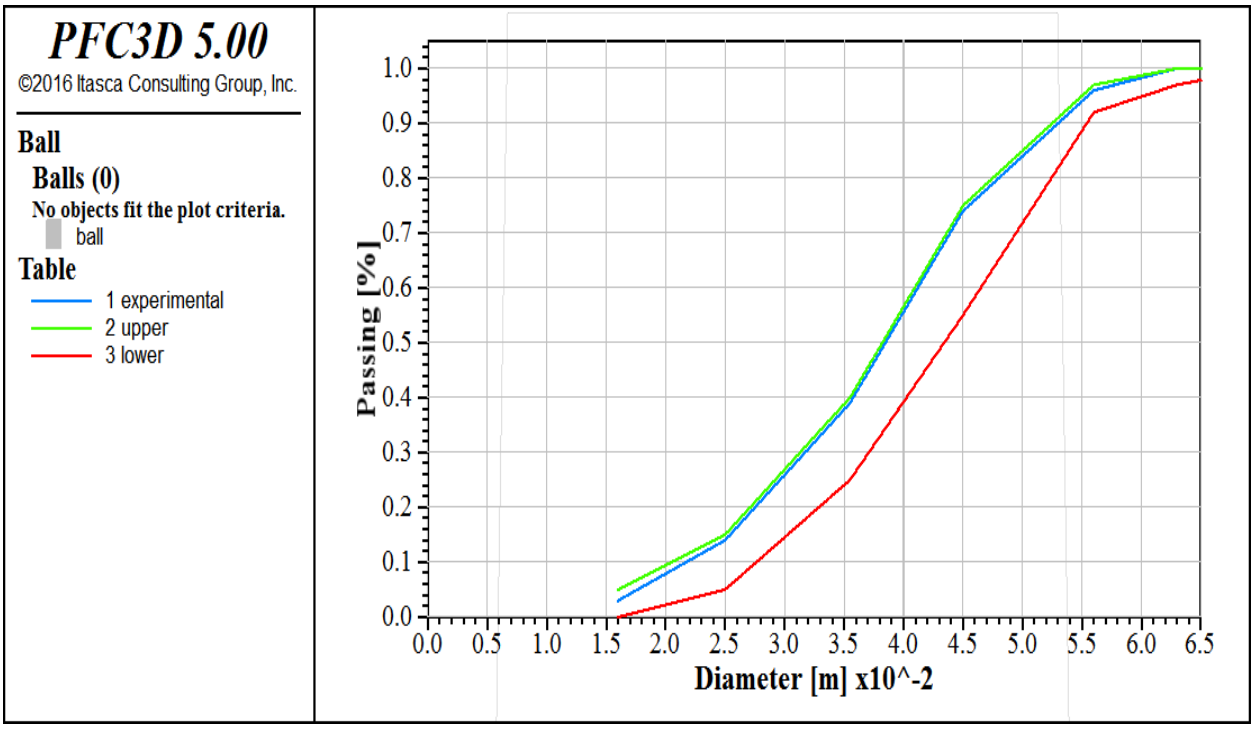

Figure 3.15: Particle Size Distribution

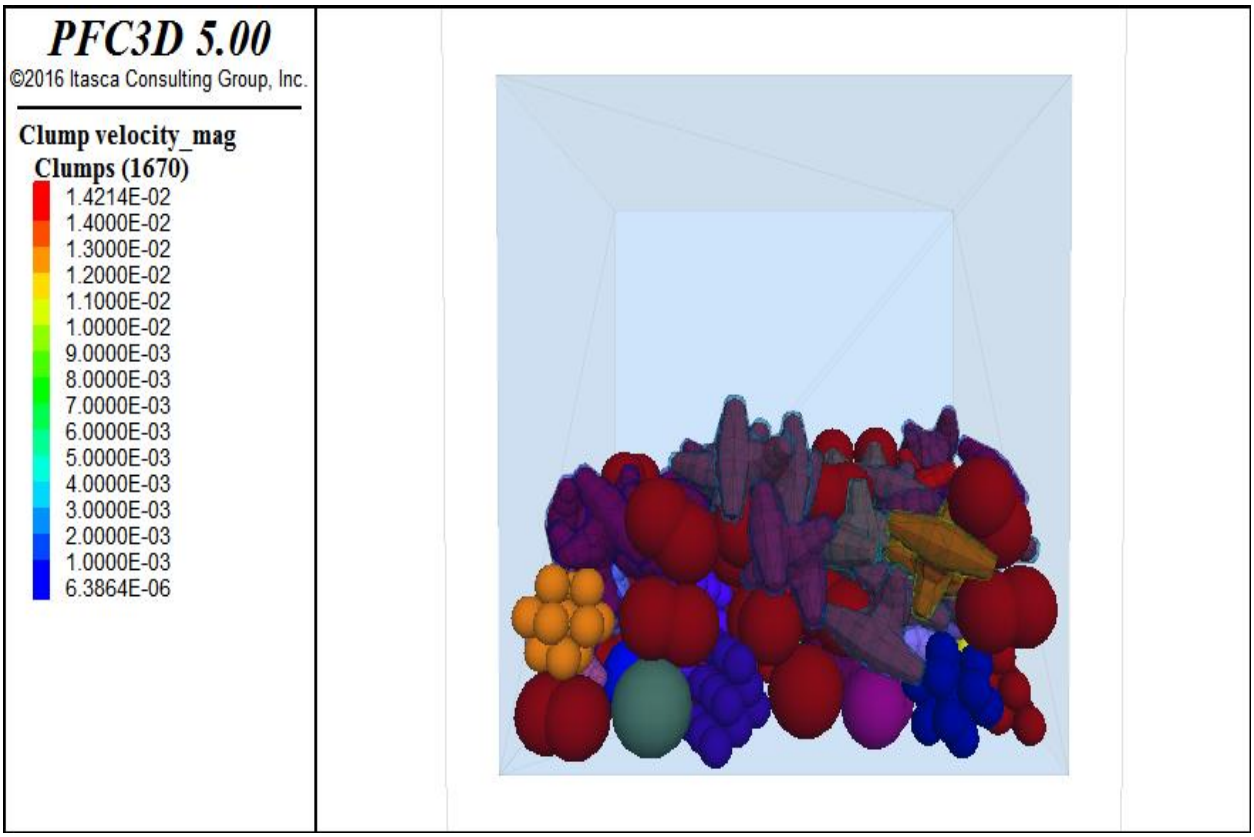

Figure 3.16: PFC3D Modeling Result

The maximum vibrational velocity is 0.014m/s as shown on the modeling which is higher than the previous result. This is due to the presence of fine particles.

3.5. Discussion

The transport of a ballast particle onto the railhead can be thought of in two stages; initial suspension of the particle and subsequent flight into the path of the wheel. The aerodynamic measurements have indicated that the across-track airflows, when coupled with the significant along-vehicle airflows close to the ballast surface and associated pressure fluctuations, could result in an airborne ballast particle being swept onto the railhead to be crushed by the wheel. The mechanical (geophone, accelerometer, and load cell) measurements showed that the ballast bed may experience significant train-induced forces, not related to aerodynamic factors, due to mechanical excitation of the track bed; and two mechanisms of ballast levitation – either a large initial velocity or a small initial velocity plus in-flight lift – were considered.

In the first case, an initial vertical velocity of about 2 m/s is required to initiate flight. This is well above that indicated by the geophone measurements, but could perhaps arise from extreme differential aerodynamic pressures over the particle. Taking the second approach, an initial vertical velocity of the order of that measured by the geophones (0.02 m/s), together with a vertical flow velocity field consistent with the maximum measured in the tests, and needs to be imposed to sustain flight. Filtered measurements of sleeper and ballast velocity and acceleration showed that the ballast particles were unlikely to have sufficient velocity to become airborne due to mechanical vibrations alone. Unfiltered ballast accelerations of up to 20 m/s^2 were measured in relatively high frequency events, but it is not thought that these would last long enough to cause ballast particles to become airborne [3].

The modeling is done with two different gradation test. The first gradation is pure aggregate and the second gradation is with some fine particles. In the first modelling the vibrational speed is 0.011m/s and the second one is 0.014m/s. This difference is due to their mass. Smaller ballasts have higher vibrational speed and exposed to ballast flying.

Generally, the vibrational speed is very small to occur ballast flying due to its ground vibration only.

The major factors of ballast flying for Addis – Adama is the following:

Operating speed

The key aerodynamic factor is speed since the aerodynamic force is proportional to the square of the speed of the train. It is the most important contribution to ballast flight risk. The speed of the Addis – Adama line project is designed to be 160km/h. Since it is double track, when the trains pass each other their speed will add up and it contribute to ballast flying with other additional factors.

Dynamic load

Several research studies have explored the behavior of ballast subjected to the dynamic load of the train. It was discovered that under certain loading conditions, the particles at the surface of the track would become weightless, meaning that the reacting forces applied to the particle would be large enough to overcome gravity. Addis – Adama project serves for passenger and freight loading and its dynamic load is high. This dynamic load will add up with other factors and it contribute additional force for the ballast flying.

Ground Effects

Sub-ballast quality

The type of material used in the sub-ballast layer might affect the amplitude of the response of the track system. A layer made by hot-mix asphalt (HMA) presents a different response than a stabilized layer made of concrete aggregate or similar types of stabilized material.

Sub-ballast layer response

A hot-mix asphalt layer presents a different dynamic response than an unbound aggregate or other stabilized material. Furthermore, one has to consider track transitions, which have an effect in terms of the differential settlement and change in the stiffness, leading to a different type of track response. There are many bridges and cut and fill sections in Addis – Adama project and these transitions have to be treated well.

Seismicity

Small magnitude earthquakes, while not felt directly by humans, can produce an input ground motion to the ballast layer and cause some vibratory effects. The vibrations may not be visible (the ballast particle may not move), but the ballast particles lying on the top layer of the ballast crib could become sensitive to the input ground motions sparked by the minor earthquake. Earthquakes of magnitude 3 or less normally do not cause a slowdown of operations, since there is not enough energy released to cause any damage to the track structure itself. However, the superposition of the input frequencies generated by both the train and the seismic activity, combined with the aerodynamic effects, may contribute to particle displacement. Addis – Adama project is in the Great Rift Valley. Records show that in this area earth quack occurred frequently and this facilitate ballast flying. Around Adama area earth quack is occurred up to 6.2 in Richter scale.

Atmospheric Conditions

High wind

While several previous researchers have studied the effect of crosswinds on the body of the train, it is important to take into account the effect of those same crosswinds on ballast structure. High winds blowing on the track could alter the arrangement of the particles laying on the surface of the track bed. This effect is particularly important with respect to smaller ballast particles present in the ballast. Addis – Adama project is highly exposed to wind force especially around Adama, because the wind speed at Adama is above 3m/s. This wind speed can change the position and arrangement of ballast.

Chapter 4

4. Conclusion and Recommendation

4.1. Conclusion

The modeling result shows the average ballast vibrational speed for Addis – Adama project condition is about 0.014m/s, which is below 0.02m/s. To lift the ballast with the wind force generated by the train, the vibrational speed has to be above 0.02m/s.

Lifting of ballast due to ballast vibration and an additional wind force created by the train due to aerodynamic force needs higher acceleration and vertical speed of the ballast. So according to the modeling result, there will not be ballast flight on the Addis – Adama project. When two trains pass each other, the aerodynamic force is higher than one train only. But the ballast bed vibration due to mechanical vibration, which is the train force, is small to lift the ballast.

Other factors like seismic activity, dynamic load, operating speed, wind force and ground condition affect highly the ballast flying property. Adama is highly exposed to earth quack and it has high wind speed. High wind speed change the stable position of the particle and leads to ballast flying. The project has also many cut and fill section and there are bridges. These also affect the ground conditions at the transition area.

This modelling mainly consider the ballast property and its load. All other factors have to be included with the aerodynamic force simultaneously and have to be studied in detail.

4.2. Recommendation

Even though there is no ballast flight on the project, some measures have to be considered.

1. Sleepers have to be clean and free from ballasts. Since sleeper vibration is much higher than ballast vibration, the sleepers have to be clean and free from ballast particles to minimize ballast lifting.
2. Bigger size ballast has to be used on the top to prevent lifting. Ballast mass is one of the factors as shown in the modeling. Smaller size ballast has higher vibration and can be easily displaced by wind and aerodynamic force.
3. Frequent maintenance of ballast is necessary. After some time ballast might degrade and contaminated. This finer particles can be lifted and trapped by the wheel and rail. It damages both the wheel and rail. To minimize lifting frequent maintenance is very mandatory. Transition sections and bridges also have to be checked frequently, especially on the bridges vibration is very high and it could be the major factor for the ballast flying.

4.3. Future work

Ballast material has to be studied well and one of the problem of ballasted track is ballast flying. To study ballast flying in depth, experimental and DEM modeling has to be used in combination. The following has to be considered.

1. Experimental data like aerodynamic force, ballast and sleeper vibration should be checked during service time.
2. DEM modeling has to be coupled with computational fluid dynamics solver to model both vibrational and aerodynamic force simultaneously.
3. If ballast flight occurs, records have to be kept for further study.

References

1. Francesco Bedini Jacobini, Erol Tutumluer, Mohd Rapik Saat (2013), "Identification of High-Speed Rail Ballast Flight Risk Factors and Risk Mitigation Strategies", 10th World Congress on Railway Research, Australia.
2. G.Q. Jing, G.X. Liu, J. Lin, J. Martinez and C.T. Yin (2014), "Aerodynamic characteristics of individual ballast particle by wind tunnel tests", Journal of Engineering Science and Technology, Beijing, China.
3. A D Quinn1, M Hayward, C J Baker, F Schmid, J A Priest, and W Powrie (2009), "A full-scale experimental and modelling study of ballast flight under high-speed trains", University of Birmingham, UK.
4. G.Q Jing, Y.D Zhou, Jian Lin, J. Zhang (2012), "Ballast flying mechanism and sensitivity factors analysis", Jiao tong University, China.
5. H.B. Kwon, C.S. Park, "An experimental study on the relationship between ballast flying phenomenon and strong wind under high speed train", Korea Railroad Research Institute, Korea.
6. Benigno J. Lazaro, Ezequiel Gonzalez, "Characterization and Modeling of Flying Ballast Phenomena in High-speed Train Lines", Madrid, Spain.
7. Le Pen, L.M. & Powrie, W. (2011), "Contribution of base, crib and shoulder ballast to the lateral sliding resistance of railway track", a geotechnical perspective. Proc. IMechE,, pp 113-128, Part F Journal of Rail and Rapid Transit.
8. Coenraad Esveld (2001), "Modern Railway Track", second Edition, Delft University of Technology.
9. Buddhima Indraratna, Wadud Salim, Cholachat Rujikiatkamjorn (2011), "Advanced Rail Geo-technology – Ballasted Track", Taylor & Francis Group, London, UK.
10. Ernest T.Selig and John M. Waters (1995), "Track geo technology and substructure management", London.
11. Wee Loon Lim, BEng (Hons) (2004), "Mechanics of Railway Ballast Behaviour", Thesis submitted to The University of Nottingham for the degree of Doctor of Philosophy.

12. GAO Liang, LUO Qi, XU Yang, JING Guo-Qing, JIANG Han-Ke (2015), "Discrete element method of improved performance of railway ballast bed using elastic sleeper", Central South University Press and Springer-Verlag Berlin Heidelberg.
13. C. CHOLET etl, "Study of the mechanical behavior of the ballast using discrete approach", France.
14. M. Lu · G. R. McDowell (2006), "The importance of modelling ballast particle shape in the discrete element method".
15. Hai Huang (2010), "Discrete element modeling of railroad ballast using imaging based aggregate morphology characterization", Dissertation submitted in partial fulfillment of the requirements for the degree of Doctor of Philosophy in Civil Engineering in the Graduate College of the University of Illinois at Urbana-Champaign, Urbana, Illinois.
16. PFC Manual (2016), Documentation for PFC Version 5.0.
17. Enad Mahmoud, A.T. Papagiannakis, David Renteria (2016), "Discrete Element Analysis of Railway Ballast under Cycling Loading", Advances in Transportation Geotechnics 3. The 3rd International Conference on Transportation Geotechnics.
18. Gilles Saussine, Charles Voivret, Nicolas Paradot and Eliane Allain (2015), "A risk assessment method for ballast flight; managing the rolling stock/infrastructure interaction", Journal of Rail and Rapid Transit.
19. Kedir Abdu (2014), "Assessment of Degradation and Performance Improvement of Railway Ballast with Geo synthetics - A Case Study of National Railway Network", AAU, Addis Ababa Ethiopia.
20. Biruk Gebremedhin (2015), "Identifying and optimizing suitable source of ballast material (Case study on Sebeta-Meiso-Dewalle railway project)", AAU, Addis Ababa Ethiopia.
21. China International Engineering Consulting Corporation (2012), "Final Evaluation Report on the Feasibility Study of Addis Ababa/Sebeta– Djibouti Railway Project", Ethiopia
22. CREC Addis Ababa –MIESO railway project (2015), "Testing report for stone ballast", Ethiopia.
23. Cheng, Nakata & Bolton (2003), "Discrete element simulation of crushable soil", pp. 633-641.

24. D.Robertson & M.D.Bolton (2001), "Discrete element simulation of crushable grains and soils", Cambridge university engineering department, United Kingdom.
25. O. Harireche, G.R. McDowell (2003), "Discrete element modelling of cyclic loading of crushable aggregates".
26. P.A. Cundall and D.L. Strack, "A discrete numerical model for granular assemblies"
27. Erol Tutumluer etl, "Field Validated Discrete Element Model for Railroad Ballast", Urbana-Champaign, University of Illinois.
28. Jose E. Andrade, Reid Kawamoto (2016), "LS-DEM: A New Paradigm for Discrete Element Simulations".
29. Li, Huiqi (2013), "Discrete element method (DEM) modelling of rock flow and breakage within a cone crusher", PhD thesis, University of Nottingham.
30. M. Lu · G. R. McDowell (2006), "The importance of modelling ballast particle shape in the discrete element method", pp. 69-80.
31. W. L. Lim · G. R. McDowell (2005), "Discrete element modelling of railway ballast", pp. 19-29.
32. Heinz Konietzky (2010), "Discrete element simulation of ballast and gravel under special consideration of grain-shape, grain-size and relative density Michael Stahl".
33. Erol Tutumluer etl (2007), "Discrete Element Modeling of Railroad Ballast Settlement", University of Illinois.
34. Stefan Luding, "Introduction to Discrete Element Methods", Netherlands.
35. Shivam Gupta (2006), "A Discrete Numerical Model For Studying Micro-Mechanical Relationship In Granular Assemblies", Indian Institute Of Technology Kanpur, India.
36. Brian Mark Parker (2009), "Simulation and Analysis of Particle Flow Through an Aggregate Stockpile".
37. David Oskar Potyondy (2015), "The bonded-particle model as a tool for rock mechanics research and application: current trends and future directions", Minneapolis, MN, USA.
38. Yu Qian, Erol Tutumluer, M. ASCE, and Hai Huang (2011), "A Validated Discrete Element Modeling Approach for Studying Geogrid-Aggregate Reinforcement Mechanisms", Washington State University, USA.

39. David Potyondy (2016), "Material-Modeling Support in PFC 5.0 FISHTank (fistPkg24)".
40. K Shiva Prashanth Kumar, M Ashok Kumar and P M B Rajkiran Nanduri (2015), "Analysis of Wind Speed Data for Energy Production at Central Ethiopia, Adama", International Journal of Recent Research in Science, Engineering and Technology, Vol 1, Issue 2.
41. Sian Herbert (2013), "Assessing seismic risk in Ethiopia".
42. Dr. Ji Shunying, "Discrete Element Modeling of Mechanical Behavior of Railway Ballast", State Key Laboratory of Structural Analysis for Industrial Equipment, Dalian University of Technology, Dalian, China.

Appendix

Source Code Used for Programming

1st Gradation

```
; fname: gradation.p3dat

;Create a balls assembly from a Particle Size Distribution

new

;Input raw data of PSD

def gradation

  global exptab = table.create('experimental')

  table(exptab,0.016) = 0.00

  table(exptab,0.025) = 0.09

  table(exptab,0.0355) = 0.37

  table(exptab,0.045) = 0.73

  table(exptab,0.056) = 0.95

  table(exptab,0.063) = 0.99

  table(exptab,0.07) = 1.0

end

@gradation

def gradation

  global exptab = table.create('upper')

  table(exptab,0.016) = 0.05
```

```
  table(exptab,0.025) = 0.15
  table(exptab,0.0355) = 0.40
  table(exptab,0.045) = 0.75
  table(exptab,0.056) = 0.97
  table(exptab,0.063) = 1.0
  table(exptab,0.07) = 1.0
end
@gradation
def gradation
  global exptab = table.create('lower')
  table(exptab,0.016) = 0.0
  table(exptab,0.025) = 0.05
  table(exptab,0.0355) = 0.25
  table(exptab,0.045) = 0.55
  table(exptab,0.056) = 0.92
  table(exptab,0.063) = 0.97
  table(exptab,0.07) = 1.0
end
@gradation
return
; eof: Gradation.p3dat
```

2nd gradation

```
; fname: gradation.p3dat

;Create a balls assembly from a Particle Size Distribution

new

;Input raw data of PSD

def gradation

  global exptab = table.create('experimental')

  table(exptab,0.016) = 0.03

  table(exptab,0.025) = 0.14

  table(exptab,0.0355) = 0.39

  table(exptab,0.045) = 0.74

  table(exptab,0.056) = 0.96

  table(exptab,0.063) = 1.0

  table(exptab,0.07) = 1.0

end

@gradation

def gradation

  global exptab = table.create('upper')

  table(exptab,0.016) = 0.05

  table(exptab,0.025) = 0.15

  table(exptab,0.0355) = 0.40
```

```
  table(exptab,0.045) = 0.75
  table(exptab,0.056) = 0.97
  table(exptab,0.063) = 1.0
  table(exptab,0.07) = 1.0
end
@gradation
def gradation
  global exptab = table.create('lower')
  table(exptab,0.016) = 0.0
  table(exptab,0.025) = 0.05
  table(exptab,0.0355) = 0.25
  table(exptab,0.045) = 0.55
  table(exptab,0.056) = 0.92
  table(exptab,0.063) = 0.97
  table(exptab,0.07) = 1.0
end
@gradation
return
; eof: Granulometry.p3dat
```

Clumps

```
;fname: mpParams-Clumped.p3dat

; Specify the material properties:

;   common, packing and material groups.

cmat default model linear property kn 5e6

cmat default type pebble-pebble model linearpbond property kn 5e6 proximity 0.1

contact method bond gap 2.0e-4

; set linear stiffness using methods

contact method deform emod 1.0e9 krat 1.0

; set stiffness of bonds using methods

contact method pb_deform emod 1.0e9 krat 1.0

; set bond strengths

contact property pb_ten 10.0e6 pb_coh 50.0e6 pb_fa 0.0

; set some damping at the contacts

contact property dp_nratio 0.5

; set pebble-pebble friction to non-zero value

contact property fric 0.577 range contact type pebble-pebble

clump template create ...

    pebcalculate ...

    name BnS ...

    pebbles 13 ...
```

0.02,-0.02,-0.011547,0.03266 ...

0.02,0.0, 0.02309401, 0.03266 ...

0.02,0.0, 0.0, 0.0 ...

0.02,-0.02,-0.034641016151378,0.0 ...

0.02,-0.04,0.0,0.0 ...

0.02,-0.02,0.034641016151378,0.0 ...

0.02,-0.02,0.011547,-0.03266 ...

0.02,0.0,-0.02309401, -0.03266 ...

0.02,0.02,0.011547,-0.03266 ...

0.02,0.02,0.034641016151378,0.0 ...

0.02,0.04,0.0,0.0 ...

0.02,0.02,-0.034641016151378,0.0 ...

0.02,0.02, -0.011547, 0.03266

clump template create ...

pebcalculate ...

name Bv1 ...

pebbles 14 ...

0.02,0.02,0.02,0.028284271247 ...

0.02,0.0, 0.0, 0.0 ...

0.02,-0.02,-0.02,-0.028284271247 ...

0.02,0.02,-0.02,-0.028284271247 ...

0.02,0.02,0.02,-0.028284271247 ...

0.02,-0.02,0.02,-0.028284271247 ...

0.02,-0.02,0.06,-0.028284271247 ...

0.02,0.0, 0.04, 0.0 ...

0.02,0.04,0.04,0.0 ...

0.02,0.02,0.06,-0.028284271247 ...

0.02,0.06,0.06,-0.028284271247 ...

0.02,0.06,0.02,-0.028284271247 ...

0.02,0.06,-0.02,-0.028284271247 ...

0.02,0.04, 0.0, 0.0

clump template create ...

pebcalculate ...

name BSnc ...

pebbles 28 ...

0.02,0.02,0.02,0.028284271247 ...

0.02,0.0, 0.0, 0.0 ...

0.02,-0.02,-0.02,-0.028284271247 ...

0.02,0.02,-0.02,-0.028284271247 ...

0.02,0.02,0.02,-0.028284271247 ...

0.02,-0.02,0.02,-0.028284271247 ...

0.02,-0.02,0.06,-0.028284271247 ...

0.02,0.0, 0.04, 0.0 ...

0.02,0.04,0.04,0.0 ...

0.02,0.02,0.06,-0.028284271247 ...

0.02,0.06,0.06,-0.028284271247 ...

0.02,0.06,0.02,-0.028284271247 ...

0.02,0.06,-0.02,-0.028284271247 ...

0.02,0.04, 0.0, 0.0 ...

0.02,0.0, 0.0, -0.096568542494 ...

0.02,-0.02,-0.02,-0.068284271247 ...

0.02,-0.02,0.02,-0.068284271247 ...

0.02,-0.02,0.06,-0.068284271247 ...

0.02,0.02,0.06,-0.068284271247 ...

0.02,0.0, 0.04, -0.096568542494 ...

0.02,0.04,0.04,-0.096568542494 ...

0.02,0.06,0.06,-0.068284271247 ...

0.02,0.06,0.02,-0.068284271247 ...

0.02,0.02,0.02,-0.068284271247 ...

0.02,0.02,-0.02,-0.068284271247 ...

0.02,0.06,-0.02,-0.068284271247 ...

0.02,0.04, 0.0, -0.096568542494 ...

0.02,0.02,0.02,-0.124852813741

```
def mpSetCommonParams
; Set common parameters.
  cm_matName = 'Ballast'
  ; ** Typical aggregate base layer of an asphalt-surface roadway (linear parallel bonded material).
  cm_matType = 0
  cm_localDampFac = 0.7
  cm_densityCode = 0
  cm_densityVal = 2650.0
  ; Grain shape & size distribution group:
    cm_shape = 1
    cm_nSD = 5
    cm_typeSD = array.create(cm_nSD)
    cm_ctName = array.create(cm_nSD)
    cm_Dlo    = array.create(cm_nSD)
    cm_Dup    = array.create(cm_nSD)
    cm_Vfrac  = array.create(cm_nSD)
    cm_ctName(1) = 'BS1'
    cm_Dlo(   1) = 16.0e-3
    cm_Dup(   1) = 25.0e-3
    cm_Vfrac( 1) = 0.09
```

```
    cm_ctName(2) = 'BS2'
    cm_Dlo(   2) = 25.0e-3
    cm_Dup(   2) = 35.5e-3
    cm_Vfrac( 2) = 0.28
    cm_ctName(3) = 'BS3'
    cm_Dlo(   3) = 35.5e-3
    cm_Dup(   3) = 45.0e-3
    cm_Vfrac( 3) = 0.36
    cm_ctName(4) = 'BS3'
    cm_Dlo(   4) = 45.0e-3
    cm_Dup(   4) = 56.0e-3
    cm_Vfrac( 4) = 0.22
    cm_ctName(5) = 'BS1'
    cm_Dlo(   5) = 56.0e-3
    cm_Dup(   5) = 63.0e-3
    cm_Vfrac( 5) = 0.05
end
@mpSetCommonParams
def mpSetPackingParams
; Set packing parameters.
  pk_Pm = 150.0e3
```

```
  pk_procCode = 0
  pk_nc = 0.43
  ; Boundary-contraction group:
    pk_fricCA = 0.0
    pk_vLimit = 1.0
end
@mpSetPackingParams
def mpSetLinParams
; Set linear material parameters.
  ; Common group (set in mpSetCommonParams)
  ; Packing group (set in mpSetPackingParams)
  ; Linear material group:
    lnm_emod = 500e6
    lnm_krat = 1.5
    lnm_fric = 0.4
end
@mpSetLinParams
@_mpCheckAllParams
@mpListMicroProps
return
;EOF: mpParams-Clumped.p3dat
```